# NASA Tech Briefs

National Aeronautics and
Space Administration

**Electronic Components and Circuits**

**Electronic Systems**

**Physical Sciences**

**Materials**

**Computer Programs**

**Mechanics**

**Machinery**

**Fabrication Technology**

**Mathematics and Information Sciences**

**Life Sciences**

00-06

2000-022965/NF C

June 2000

# INTRODUCTION

Tech Briefs are short announcements of innovations originating from research and development activities of the National Aeronautics and Space Administration. They emphasize information considered likely to be transferable across industrial, regional, or disciplinary lines and are issued to encourage commercial application.

## Availability of NASA Tech Briefs and TSPs

Requests for individual Tech Briefs or for Technical Support Packages (TSPs) announced herein should be addressed to

**National Technology Transfer Center**
Telephone No. **(800) 678-6882** or via World Wide Web at **www2.nttc.edu/leads/**

Please reference the control numbers appearing at the end of each Tech Brief. Information on NASA's Commercial Technology Team, its documents, and services is also available at the same facility or on the World Wide Web at **www.nctn.hq.nasa.gov**.

Commercial Technology Offices and Patent Counsels are located at NASA field centers to provide technology-transfer access to industrial users. Inquiries can be made by contacting NASA field centers and program offices listed below.

## NASA Field Centers and Program Offices

**Ames Research Center**
*Carolina Blake*
*(650) 604-1754 or*
*cblake@mail.arc.nasa.gov*

**Dryden Flight Research Center**
*Lee Duke*
*(805) 258-3802 or*
*lee.duke@dfrc.nasa.gov*

**Goddard Space Flight Center**
*George Alcorn*
*(301) 286-5810 or*
*galcorn@gsfc.nasa.gov*

**Jet Propulsion Laboratory**
*Merle McKenzie*
*(818) 354-2577 or*
*merle.mckenzie@jpl.nasa.gov*

**Johnson Space Center**
*Hank Davis*
*(281) 483-0474 or*
*henry.l.davis1@jsc.nasa.gov*

**John F. Kennedy Space Center**
*Gale Allen*
*(407) 867-6226 or*
*gale.allen-1@ksc.nasa.gov*

**Langley Research Center**
*Sam Morello*
*(757) 864-6005 or*
*s.a.morello@larc.nasa.gov*

**Glenn Research Center**
*Larry Viterna*
*(216) 433-3484 or*
*cto@grc.nasa.gov*

**George C. Marshall Space Flight Center**
*Sally Little*
*(256) 544-4266 or*
*sally.little@msfc.nasa.gov*

**John C. Stennis Space Center**
*Kirk Sharp*
*(228) 688-1929 or*
*technology@ssc.nasa.gov*

**NASA Program Offices**
At NASA Headquarters there are seven major program offices that develop and oversee technology projects of potential interest to industry:

**Carl Ray**
*Small Business Innovation Research Program (SBIR) & Small Business Technology Transfer Program (STTR)*
*(202) 358-4652 or*
*cray@mail.hq.nasa.gov*

**Dr. Robert Norwood**
*Office of Commercial Technology (Code RW)*
*(202) 358-2320 or*
*rnorwood@mail.hq.nasa.gov*

**John Mankins**
*Office of Space Flight (Code MP)*
*(202) 358-4659 or*
*jmankins@mail.hq.nasa.gov*

**Terry Hertz**
*Office of Aero-Space Technology (Code RS)*
*(202) 358-4636 or*
*thertz@mail.hq.nasa.gov*

**Glen Mucklow**
*Office of Space Sciences (Code SM)*
*(202) 358-2235 or*
*gmucklow@mail.hq.nasa.gov*

**Roger Crouch**
*Office of Microgravity Science Applications (Code U)*
*(202) 358-0689 or*
*rcrouch@hq.nasa.gov*

**Granville Paules**
*Office of Mission to Planet Earth (Code Y)*
*(202) 358-0706 or*
*gpaules@mtpe.hq.nasa.gov*

NASA TechBriefs

National Aeronautics and
Space Administration

June 2000
00-06

5 Electronic Components and Circuits

17 Electronic Systems

23 Physical Sciences

29 Materials

33 Machinery

37 Mathematics and Information Sciences

This document was prepared under the sponsorship of the National Aeronautics and Space Administration. Neither the United States Government nor any person acting on behalf of the United States Government assumes any liability resulting from the use of the information contained in this document, or warrants that such use will be free from privately owned rights.

4

BLANK PAGE

# Electronic Components and Circuits

## Hardware, Techniques, and Processes


7 Resonant Crackwires for In Situ Monitoring of Jet Engines
8 Circuit Generates Rotation Signal From a Vibratory Gyroscope
9 Vibration-Regulating Circuit for a Mechanical Resonator
10 *Q*-Compensation Circuit for a Planar Vibratory Microgyroscope
10 Motion-Measuring Circuit for a Vibratory Capacitive Sensor
11 Inexpensive Packaged Subharmonic Down-Converter MMICs
12 Cadmium Zinc Telluride Detectors for Imaging of Gamma Rays
13 Power Supply for Miniature Quadrupole Mass Spectrometer
14 RS-232-to-Infrared Transceiver

6

BLANK PAGE

# Resonant Crackwires for In Situ Monitoring of Jet Engines

Early detection of fatigue cracks could save lives and reduce costs.

*John H. Glenn Research Center, Cleveland, Ohio*

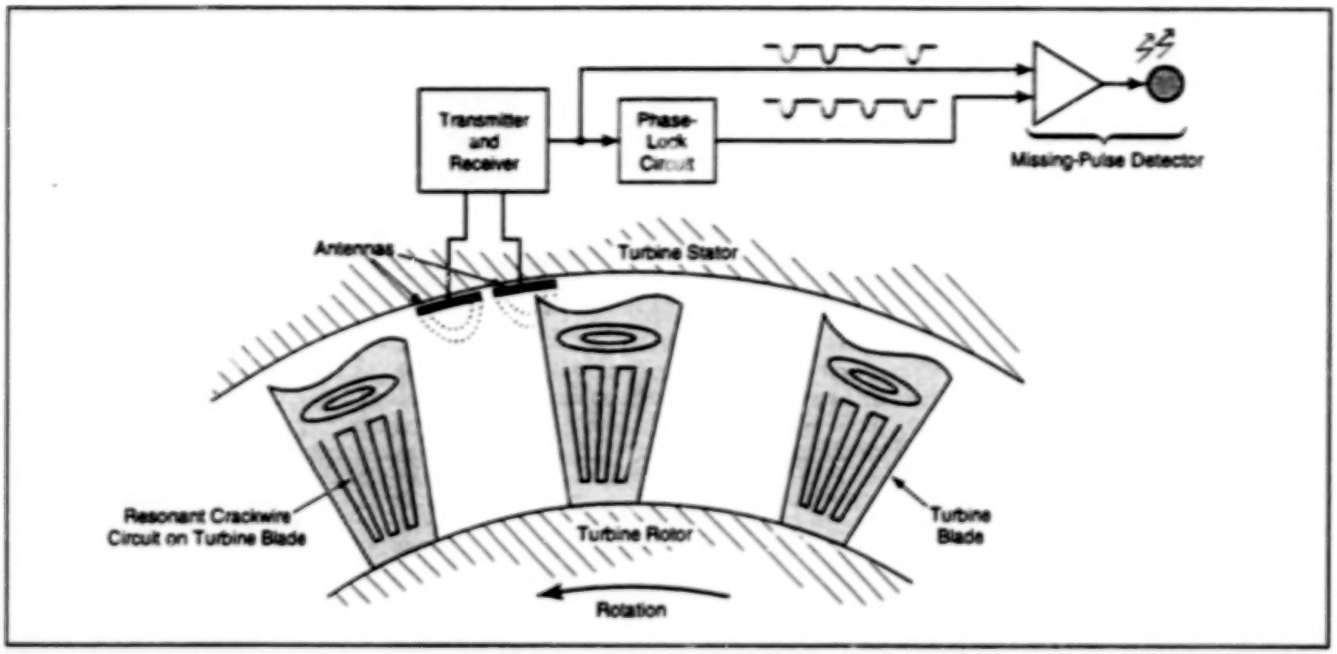


**Figure 1. Resonant Crackwire Circuits** would be bonded to the surfaces of turbine blades. In this example, the crackwire circuits on all the blades would resonate at the same frequency, so that each one would be expected to respond with a pulse when it passed by a transmitting/receiving antenna operating at that frequency. If the circuit on a passing blade were not to respond, a crack alarm for that blade would be triggered.

Fatigue cracks and plastic deformation of parts in jet aircraft engines could be detected, even during engine operation, by use of proposed *in situ* monitoring devices called "wireless resonant crackwires." Inasmuch as uncontained turbine failures are the leading engine-related hazards for aircraft, early detection of cracks and/or the associated plastic deformation could enable pilots to respond in time to save lives and limit damage. The use of wireless resonant crackwires could also reduce the costs of inspecting engines for fatigue cracks: Often, cracking occurs in engine parts that are accessible only through disassembly of engines. In many cases, the costs of disassembly and reassembly far exceed the costs of inspection, and the disassembly and reassembly processes can cause new damage.

The term "wireless resonant crackwire" is not oxymoronic, though it may appear so at first. "Wireless" as used here represents the absence of wire connections with external equipment and the use of radio signals to interrogate the crackwires.

The principle of operation of wireless resonant crackwires would be an extension of that of radio-frequency (RF) security tags attached to merchandise in some department stores. These tags contain circuits

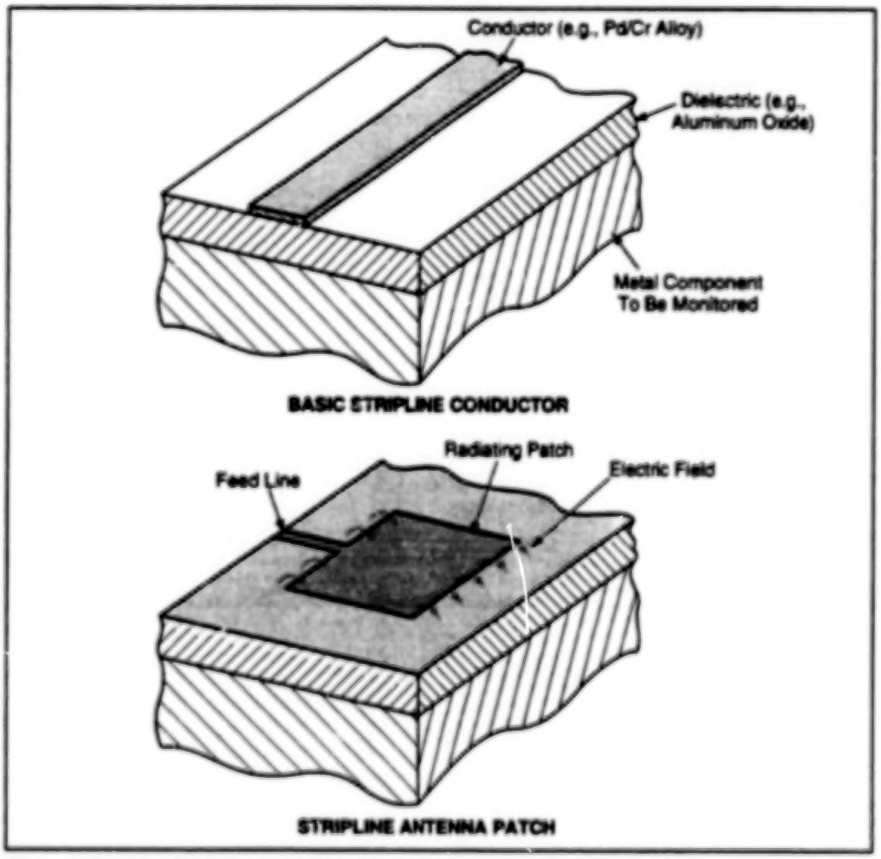


**Figure 2. Stripline Design** would likely be used for a resonant crackwire circuit on a metal component because it would be compatible with the conductivity of the component and the thin-film nature of crackwire circuitry.

that resonate at frequencies in the vicinity of 9 MHz. Upon leaving a store, a customer must pass by a large loop antenna that emits a signal swept in frequency over a range that includes the resonance frequencies of the security tags. If a security tag has not been deactivated, then it responds to the incident RF signal by ringing and reradiating at its resonance frequency. A second antenna picks up the reradiated signal, and the antenna output triggers an alarm.

To enable the customer to carry the merchandise out of the store without triggering the alarm, a clerk deactivates the tag. Deactivation is accomplished at the store checkout counter by placing the tag on a small antenna that exposes the tag to an overload-level replica of the exit signal in order to burn out a fusible link in the tag circuit. The removal of the link either makes the circuit nonresonant or else moves the resonance to a frequency outside the range of the security equipment.

Resonant crackwires would be bonded to the surfaces of such critical jet-engine components as turbine blades (see Figure 1). Like department-store security tags, resonant crackwires would include links designed to be broken to alter RF resonances. However, these links would not be broken by overload signals; instead, they would be broken by the development of cracks and/or plastic deformation in the engine components to which they were bonded. Thus, if a resonant crackwire monitored by use of a suitable transmitter, antennas, and receiver were to stop resonating at its "installed" resonance frequency, a crack alarm would be triggered.

Of course, because of the unique characteristics of the jet-engine environment (especially high temperature and the metallic nature of the components to be monitored), the design and fabrication of resonant crackwires would differ markedly from those of department-store RF security tags. Resonant crackwire circuits would likely be fabricated by use of techniques developed previously for strain gauges for monitoring engine parts at high temperatures; this would involve the deposition, on the engine parts to be monitored, of thin oxide films as dielectrics and patterned thin films of high-temperature alloys as inductors, electrodes for capacitors, and antennas. The resonance frequencies of these circuits would range upward from several hundred megahertz and possibly into the gigahertz region. In many cases that would involve monitoring of metal components, it may prove necessary to resort to stripline circuit designs, utilizing the underlying monitored components as the ground planes of stripline antennas and resonators (see Figure 2).

*This work was done by Bruce McKee, Scott Dahl, and Kathy Shkarlet of Innovative Dynamics, Inc., for* **Glenn Research Center**. *Further information is contained in a TSP [see page 1].*

*Inquiries concerning rights for the commercial use of this invention should be addressed to NASA Glenn Research Center, Commercial Technology Office, Attn: Steve Fedor, Mail Stop 4–8, 21000 Brookpark Road, Cleveland, Ohio 44135. Refer to LEW-16758.*

## Circuit Generates Rotation Signal From a Vibratory Gyroscope

Rotation is measured in terms of a difference between two vibrational velocities.

*NASA's Jet Propulsion Laboratory, Pasadena, California*

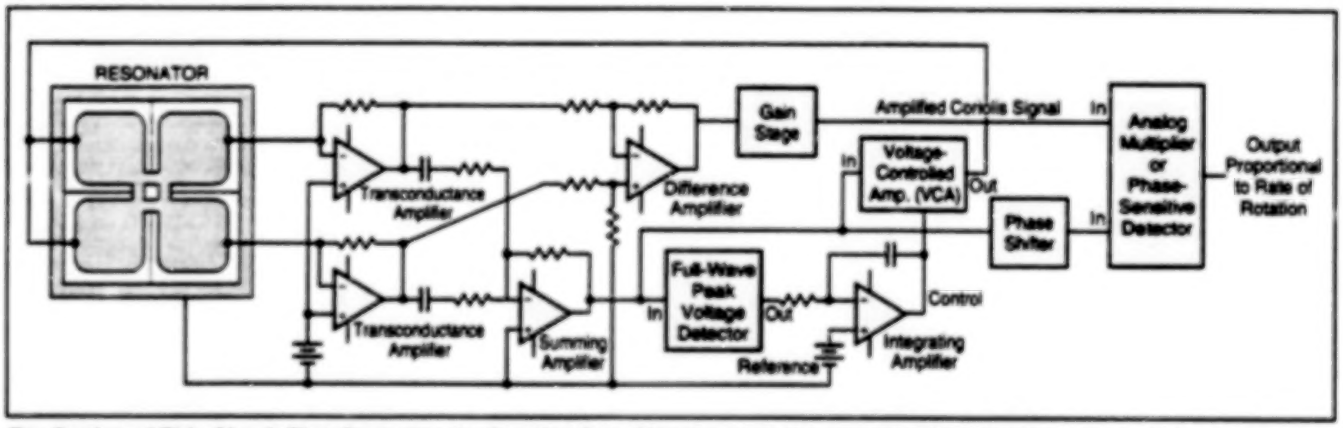


**The Portion of This Circuit That Generates the Rotation-Rate Signal** exploits the sum and difference of the outputs of the transconductance amplifiers. The difference signal is either multiplied by, or detected synchronously with respect to, the sum signal.

This is the first of four articles that address various issues concerning the generation and utilization of electronic signals in the operation of micromachined planar vibratory microgyroscopes and other sensory devices that include electrostatically actuated, capacitively sensed mechanical resonators. The subject of this article is that part of the overall electronic circuitry of a planar vibratory gyroscope that generates a signal proportional to the rate of rotation.

Some background information is prerequisite to a description of this circuitry and to the descriptions of the circuits described in the following three articles. Various aspects of micromachined planar vibratory microgyroscopes have been described in a number of previous articles in *NASA Tech Briefs*. The basic principle of operation is as follows: Four planar silicon plates are connected together by silicon springs in a symmetrical pattern resembling a clover leaf. The silicon springs lie at the center of the pattern. When in equilibrium (not vibrating), all plates lie in the same plane.

Together, the plates and springs constitute a mechanical resonator characterized by two orthogonal degenerate modes of vibration. Two of the plates are driven electrostatically to generate oscillations in one of these modes, denoted the driven mode. The oscillatory displacements or velocities of all four plates are measured by use of capacitive sensors.

One seeks to measure rotation about the axis perpendicular to the equilibrium plane of the resonator plates. The Coriolis force associated with this rotation couples energy from the driven mode to the other mode, denoted the sensing mode, in which there is a difference between the velocities of the two plates that are not driven electrostatically (the sensing

plates). This difference between velocities gives rise to a corresponding difference between the outputs of the capacitive sensors for the sensing plate. The difference signal, called the "Coriolis signal," is proportional to (1) the amplitude of oscillation of the driven plates; (2) the rate of rotation, $\Omega$; and (3) the resonance quality factor, $Q$, which is inversely proportional to the rate of damping of vibrations.

The circuitry in question is designed to generate a signal proportional to the Coriolis signal and thus to $\Omega$. This circuitry is part of the overal circuit shown in the figure. As explained in more detail in the following article, the inputs to the transconductance amplifiers are the raw velocity signals from the sensing-plate capacitors. Thus, the difference between the outputs of the two transconductance amplifiers contains the desired information.

Because of common-mode rejection, the sum of transconductance-amplifier outputs, which is proportional to the driven-mode velocity signal, contains no information on $\Omega$. If the magnitude of oscillation is held constant as described in the following article, then the sum signal has a constant magnitude. In any event, the sum signal is used as a reference for phase-sensitive detection of the difference signal. In one version of this circuitry, the difference signal is multiplied by a 90°-phase-shifted replica of the sum signal. In another version, the difference signal is synchronously detected, using the phase-shifted sum signal as the timing reference. In either version, the time-averaged output signal is proportional to $\Omega Q$.

*This work was done by Christopher Stell, Vatché Vorperian, Roman Gutierrez, and Tony Tang of Caltech for* **NASA's Jet Propulsion Laboratory**. *Further information is contained in a TSP [see page 1].*
*NPO-20097*

## Vibration-Regulating Circuit for a Mechanical Resonator

A two-loop feedback system maintains constant magnitude of vibration.

*NASA's Jet Propulsion Laboratory, Pasadena, California*

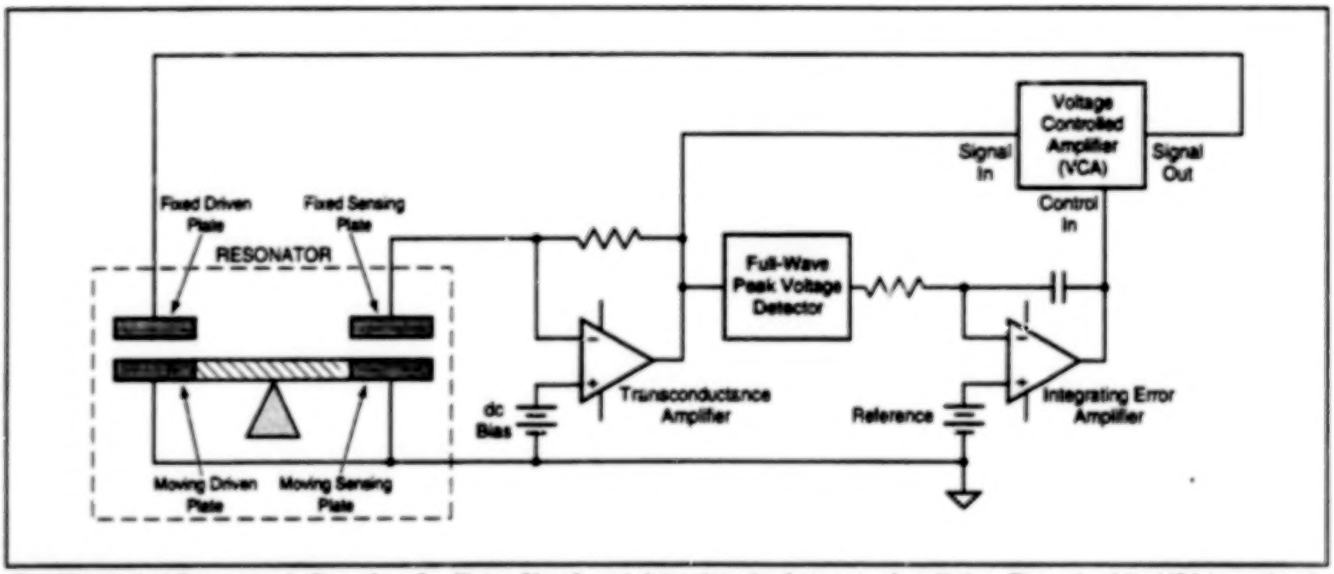


**The Mechanical Resonator Is Part of an Oscillator Circuit and determines the frequency of oscillation. The gain of the VCA is continually adjusted to regulate the magnitude of the capacitively sensed mechanical oscillations.**

The figure illustrates an improved electronic circuit that excites constant-magnitude vibrations in an electrostatically actuated, capacitively sensed mechanical resonator. The circuit can be adapted, for example, to a planar vibratory microgyroscope like that described in the preceding article.

Mounted on the moving part of the resonator are two electrodes — the driven and the sensing plates — that face corresponding fixed driven and sensing plates. Each pair of electrodes serves as a capacitor; the driven one for electrostatically exciting vibrations, the sensing one for measuring the vibrational velocity. Through the negative-feedback path of the transconductance amplifier, the fixed sensing plate becomes charged up to the dc bias applied to the "+" terminal of the transconductance amplifier. As the resonator vibrates, the voltage across the sensing capacitor thus remains constant, although its capacitance varies at a rate proportional to the vibrational velocity. By the fundamental relationship among capacitance, voltage, and charge, a current proportional to the vibrational velocity must therefore flow between the sensing plate and the "-" input of the transconductance amplifier. As a result, the transconductance amplifier puts out a voltage proportional to the vibrational velocity.

The output of the transconductance amplifier is fed to the signal-input terminal of the voltage-controlled amplifier (VCA) and to the input terminal of the full-wave peak detector. The integrating amplifier produces an error signal that is the integral of the difference between (1) the peak-detector output (which is proportional to the magnitude of the vibrational velocity) and (2) the reference voltage, which represents a desired magnitude of vibration. The error signal is fed to the control-input terminal of the VCA. The output of the VCA is proportional to the velocity and is fed back to the fixed drive plate. With sufficient gain in the amplifiers, the resonator and feedback loop oscillate together. When the amplitude of oscillation is too high or too low, the error signal adjusts the gain of the VCA to drive the magnitude of vibration toward the desired value represented by the reference voltage.

*This work was done by Christopher Stell, Vatché Vorperian, Roman Gutierrez, and Tony Tang of Caltech for* **NASA's Jet Propulsion Laboratory**. *Further information is contained in a TSP [see page 1].*
*NPO-20088*

# Q-Compensation Circuit for a Planar Vibratory Microgyroscope

The amplitude of the resonator-drive waveform is used to make the output independent of Q.

*NASA's Jet Propulsion Laboratory, Pasadena, California*

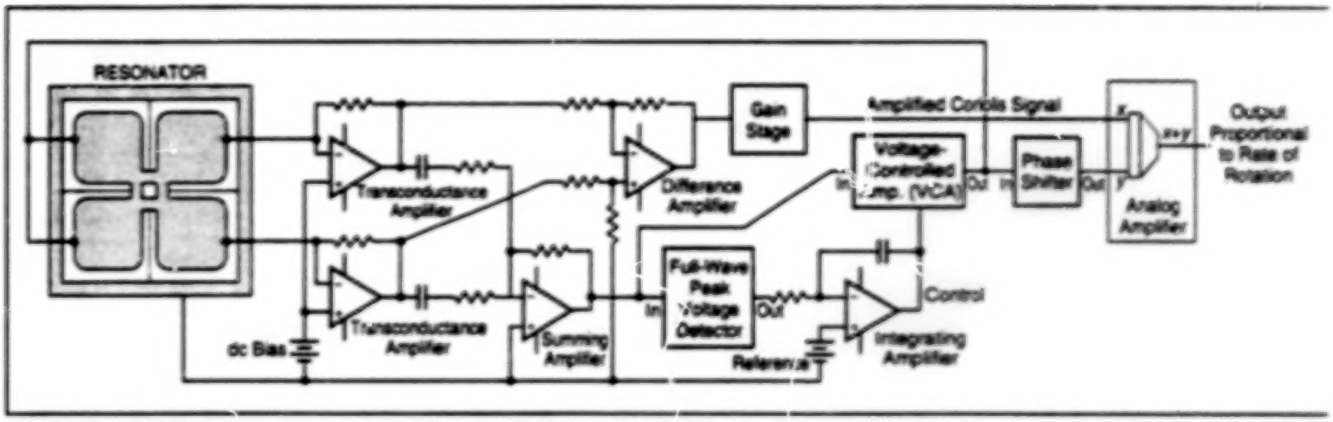


**The Portion of This Circuit That Compensates for Variations in *Q*** exploits the drive voltage generated elsewhere in the circuit. The amplitude of this drive voltage is proportional to *Q*, while the amplitude of the Coriolis signal is proportional to $\Omega Q^{-1}$. The output of the analog multiplier is proportional to the two amplitudes and thus proportional to $\Omega$, regardless of the value of *Q*.

Electronic circuitry has been devised to compensate for variations in the resonance quality factor (*Q*) of a planar vibratory microgyroscope like that described in the first of the two preceding articles. That is, the circuit makes the scale factor of the gyroscope (the factor of proportionality between the rate of rotation, $\Omega$, and the output signal) independent of *Q*.

If the Coriolis signal were to constitute the output signal, then the scale factor would be proportional to the amplitude of the input displacement and to *Q*. The amplitude of the input displacement is maintained constant by the technique described in the immediately preceding article, "Vibration-Regulating Circuit for a Mechanical Resonator," (NPO-20088). However, the rate of damping, and thus *Q*, does not remain constant; the rate of damping is very sensitive to the density and pressure of the fluid in which the resonator is immersed. Thus, there is need for further processing of the Coriolis signal through circuitry like that described below to make the scale factor remain constant despite variations in *Q*.

The circuitry in question is part of the overall electronic circuit shown in the figure. To maintain a constant input vibration amplitude, it is necessary to drive the resonator with a voltage proportional to *Q*. Other parts of the circuit generate such a drive voltage, which is applied not only to the resonator but also to the input terminal of a 90° phase shifter. The output of the phase shifter is fed to one of two input terminals of an analog multiplier. An amplified version of the Coriolis signal is applied to the other input terminal of the analog amplifier. Because the Coriolis signal is approximately 90° out of phase with the drive signal, it is approximately in phase with the output of the phase shifter. Therefore, the time-averaged output of the analog multiplier is proportional to the amplitude of the Coriolis signal (proportional to $\Omega Q$) and to the amplitude of the drive signal (proportional to $Q^{-1}$). Thus, the output of the analog multiplier is proportional to $\Omega$ only, as desired, regardless of variations in *Q*.

*This work was done by Christopher Stell, Vatché Vorperian, Roman Gutierrez, and Tony Tang of Caltech for* **NASA's Jet Propulsion Laboratory**. *Further information is contained in a TSP [see page 1].*
*NPO-20089*

# Motion-Measuring Circuit for a Vibratory Capacitive Sensor

This circuit offers some advantages over circuits designed previously for the same purpose.

*NASA's Jet Propulsion Laboratory, Pasadena, California*

The figure illustrates an improved electronic circuit that generates a signal proportional to either the instantaneous vibrational velocity or the instantaneous position (equivalently, the instantaneous vibrational displacement) of a vibratory capacitive sensor of the type discussed in the three preceding articles. This circuit offers some advantages over circuits designed previously for the same purpose; in particular, there is no need for a reference capacitor, and the circuit is insensitive to capacitive loading of its sensing amplifier.

The vibratory sensor includes a resonator equipped with capacitor electrodes in a manner similar to that of the vibration-regulating scheme described in second preceding article: Mounted on the moving part of the resonator are two electrodes — the driven and sensing plates — that face corresponding fixed driven and sensing plates. Each pair of electrodes serves as a capacitor; the driven one for electrostatically exciting vibrations, the sensing one for measuring the vibrational displacement or velocity.

Also as in the vibration-regulating scheme, the negative-feedback path of the transconductance amplifier is utilized to maintain the fixed sensing plate at a voltage equal to the dc bias applied to the "+" terminal of the transconductance amplifier. Therefore, in the absence of additional vibratory and/or electronic inputs, this circuit behaves similarly to the corresponding part of the vibration-regulating circuit; namely, the instantaneous output of the transconductance

amplifier is a voltage proportional to the instantaneous vibrational velocity.

Additional vibratory/electronic input is necessary to obtain a position signal. In particular, a voltage alternating at a frequency much greater than that of the vibration to be measured is applied to the driven plates to excite a superimposed sinusoidal vibration much smaller than the vibration to be measured. This small, high-frequency vibration gives rise to a velocity signal in the manner described above. The capacitance varies with the position of the sensing plate in a known way, and the magnitude of the velocity signal varies in proportion to the change in capacitance. Thus, the instantaneous magnitude of the velocity signal serves as an indicator of the instantaneous position of the sensing plate.

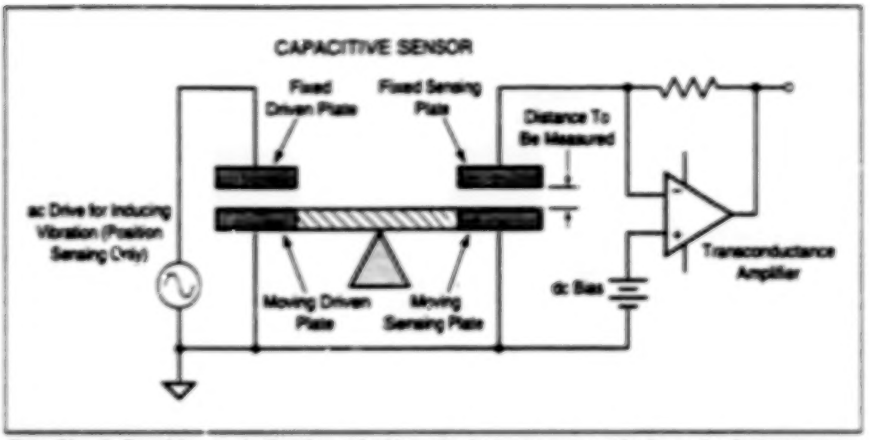


**This Circuit Provides an Indication of either the instantaneous velocity or the instantaneous position of the sensing plate, depending on the choice of operational mode as described in the text.**

*This work was done by Christopher Stell and Vatché Vorperian of Caltech for* **NASA's Jet Propulsion Laboratory.**

*Further information is contained in a TSP [see page 1].*
*NPO-20086*

## Inexpensive Packaged Subharmonic Down-Converter MMICs

MMICs like these could be used in microwave digital communication receivers.

*John H. Glenn Research Center, Cleveland, Ohio*

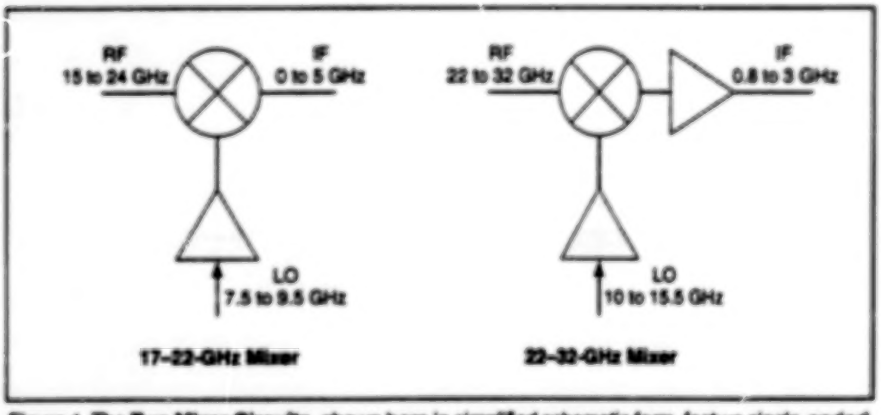


**Figure 1. The Two Mixer Circuits, shown here in simplified schematic form, feature single-ended configurations that minimize size. Inexpensive filters (not shown here) provide the needed isolation among the different frequencies.**

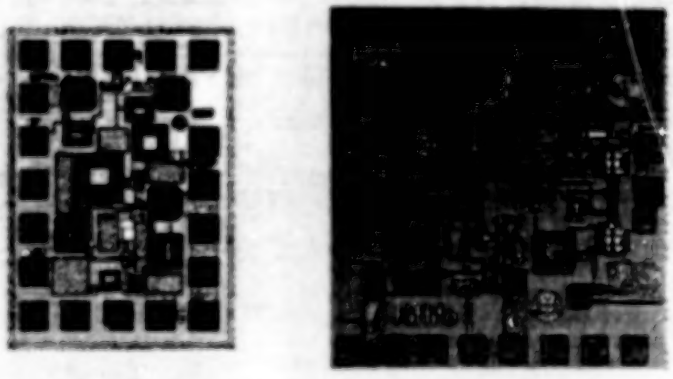


**Figure 2. The Two MMIC Chips are compact: The 17–20-GHz chip has an area of 0.7 mm$^2$; the 22–32-GHz chip has an area of 1.25 mm$^2$.**

Two packaged monolithic microwave integrated-circuit (MMIC) mixers have been designed to operate as subharmonically pumped frequency down-converters in receivers of satellite- or ground-based digital communication systems. One operates a radio frequency (RF) between 17 and 20 GHz, the other at an RF between 22 and 32 GHz (see Figure 1). These MMICs are of a type described in "MMIC Converters for K- and Ka-Band Communications" (LEW-16752), *NASA Tech Briefs*, Vol. 23, No. 7 (July 1999), page 59. The approach taken in developing this type of MMIC is one of minimizing costs by relying on well established design practices and mature, commercially available processes for fabrication of MMIC chips.

Both mixers incorporate onboard local-oscillator (LO) amplifiers to reduce the required LO drive levels. The 22–32-GHz mixer also incorporates an output [intermediate-frequency (IF)] amplifier. To reduce the sizes and thus the costs of the mixer chips, both mixers incorporate lumped circuit elements for matching of impedances (in contradistinction to the transmission-line impedance-matching elements customarily used for microwaves).

The specific practices and processes chosen for design and fabrication of the 17–20-GHz MMIC are those of GaAs metal/semiconductor field-effect transistors (MESFETs) with 0.5-μm design rules, while those of electron-acceptor-doped high-electron-mobility transistors (p-HEMTs) with

0.25-μm design rules were chosen for the 22–32-GHz MMIC. Figure 2 depicts the two MMIC chips. Both MMIC chips are integrated into ball-grid-array (BGA) packages, which are leadless ceramic interconnection substrates with tungsten/copper vias; the MMICs are inserted in these packages in surface-mount configurations and bonded in place by use of arrays of noncollapsing, hard balls made of a copper/silver eutectic alloy.

In tests, the 17–20-GHz down-converter was found to perform well at RFs from 15 to 24 GHz, LO frequencies of 7 to 10.5 GHz, and IFs from 0 to 5 GHz. The 22–32-GHz down-converter was found to perform well over the RF range from 22 to 32 GHz in tests in which the LO frequency was swept, along with the RF, to maintain an IF of 2 GHz.

*This work was done by Paul Blount of Hittite Microwave Corp. for* **Lewis Research Center**. *Further information is contained in a TSP [see page 1].*

*Inquiries concerning rights for the commercial use of this invention should be addressed to NASA Glenn Research Center, Commercial Technology Office, Attn: Steve Fedor, Mail Stop 4–8, 21000 Brookpark Road, Cleveland, Ohio 44135. Refer to LEW-16805.*

## Cadmium Zinc Telluride Detectors for Imaging of Gamma Rays

Angular resolution less than an arc minute can be achieved.

*Goddard Space Flight Center, Greenbelt, Maryland*

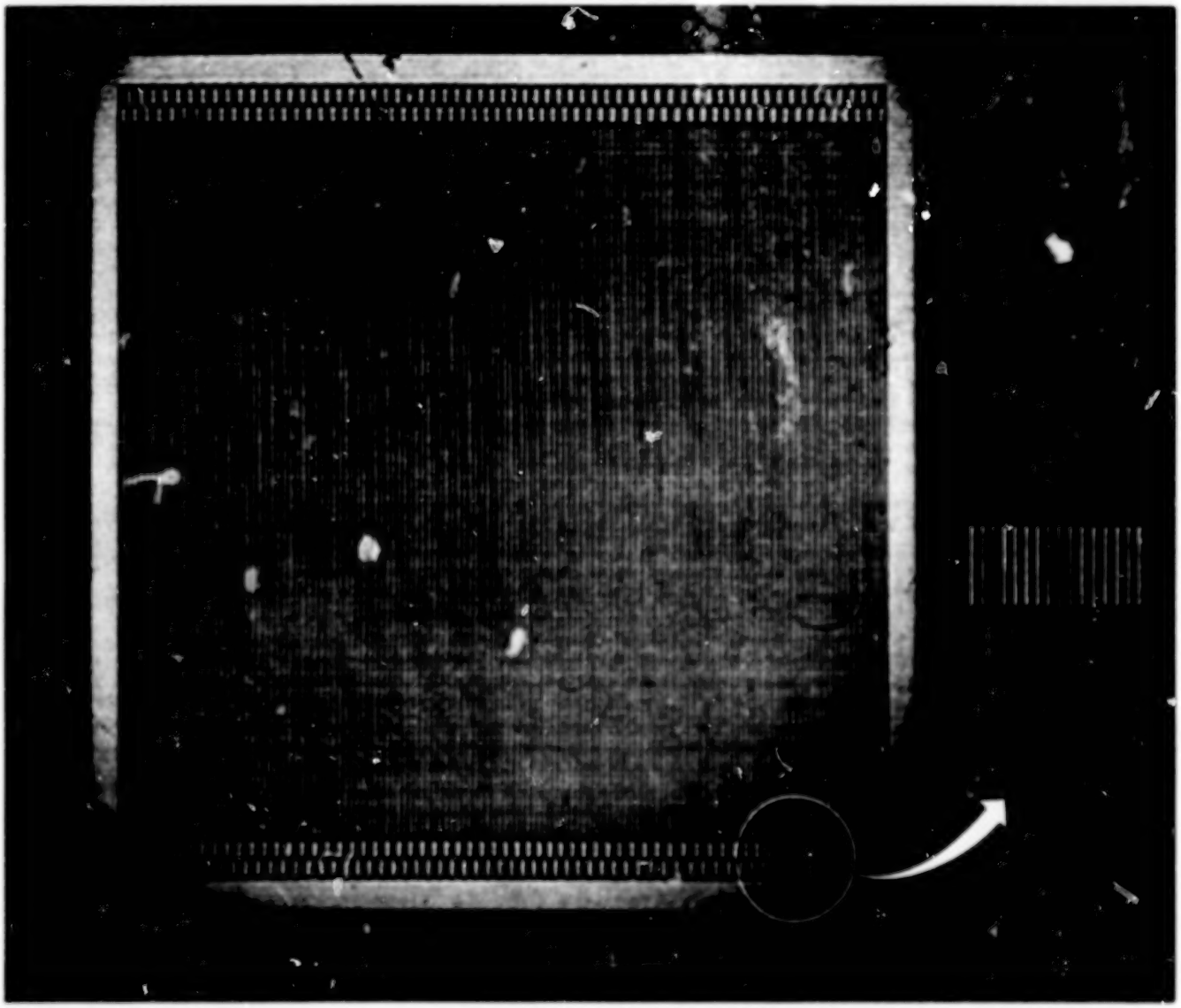

**Detector Modules** like this one are arranged in a square array to form a sensor for imaging of hard x rays and γ rays. A pixel pitch of 100 μm in two dimensions is defined by orthogonal arrays of detector strips on the upper and lower faces of each module.

Planar arrays of cadmium zinc telluride photodetectors with readout electronic circuitry have been developed for use as hard-x-ray and γ-ray image sensors. When a coded, x-and-γ-ray-opaque aperture mask is positioned in front of such a sensor, the resulting assembly is an instrument that can be used to observe hard-x-ray and γ-ray sources. In operation, the spatial pattern of x and γ rays impinging on the sensor is deconvolved from the aperture pattern to obtain an image of the source. With suitable choice of the sensor pixel pitch, coded aperture pattern, and distance of the aperture in front of the detector array, it should be possible to image radiation sources at angular resolutions of 30 arc seconds and finer. In the original

intended application, the instrument will be operated in outer space to measure precisely the directions to distant sources of hard-x-ray and γ-ray bursts that are of cosmological interest. The instrument can also be used to image hard-x-ray and γ-ray sources in a terrestrial laboratory setting; indeed, a prototype of the instrument has been demonstrated in such a setting.

Prototype sensors containing 2 × 2 and 6 × 6 arrays of detector modules made from $Cd_{0.9}Zn_{0.1}Te$ have been constructed (see figure). The dimensions of a module are 15 by 15 by 2 mm. Each face of a module is patterned with 127 metal strips, each 50 μm wide, at a pitch of 100 μm. The strip pattern is surrounded by a 450-μm guard ring. The metal strips divide the module into, and serve as electrical contacts for, a corresponding pattern of strip detectors. The strips on the front and back faces are made orthogonal to each other to establish a square pixel grid with a pitch of 100 μm.

The row and column metal strips that are collinear with each other in the various modules are electrically tied together with wire bonds to make long strips that span the entire array of modules, thereby defining a pixel coordinate grid over the whole array. The row and column strips are biased via monolithic resistors formed in voltage-divider configurations along two orthogonal edges of the array. For readout, the strips are ac-coupled, via 1,000-pF capacitors, to high-density application-specific integrated circuits.

In operation, the $Cd_{0.9}Zn_{0.1}Te$ material absorbs photons with energies between 10 and 150 keV. The electrons and holes generated in the absorption of photons drift to the anode and cathode strips, respectively, where they are collected. The charges collected on orthogonal anode and cathode strips indicate the magnitudes and positions of photon-impingement events in the detector plane. Because the cloud of drifting charges induced by each photon has a finite size and can diffuse outward as the carriers drift, charge is typically induced on three adjacent strips at 100-μm pitch. The position of impingement is determined from the average of the strip numbers weighted by the charges induced on the affected strips. In addition, the charges on affected adjacent strips must be summed for accuracy in determining the photon energy. For even greater accuracy, it is necessary to sum the signals from anode strips because the charges collected on cathode strips are reduced because of the poor hole-transport properties of $Cd_{0.9}Zn_{0.1}Te$.

Using 60-keV γ rays from a $^{241}Am$ source, a 2 × 2 prototype sensor was tested in conjunction with a 40-μm-thick gold aperture mask patterned in a 100-μm-pitch square grid supported by a 1-mm-thick beryllium substrate. The aperture mask was placed 32 mm in front of the sensor (in the fully developed instrument, the mask would be placed 800 mm in front of the sensor). The results of the test revealed that the prototype instrument was capable of an angular resolution of about 30 arc seconds. The results give confidence in computer simulations that predict that the fully developed instrument will be able to locate about 90 γ-ray bursts per year to an accuracy of ±3 arc seconds, and to produce an all-sky survey with a resolution of 30 arc seconds.

*This work was done by L. Barbier, N. Gehrels, B. Teegarden, A. M. Parsons, L. M. Bartlett, P. K. Shu, and J. Tueller of* **Goddard Space Flight Center**; *C. M. Stahle of Orbital Sciences Corp.; Z. Q. Shi, K. Hu, and S. J. Snodgrass of Hughes STX Corp.; D. M. Palmer, S. D. Barthelmy, and J. Kitaeinic of Universities Space Research Association; S. J. Lehtonen and K. J. Mach of Johns Hopkins University Applied Physics Laboratory; P. Kurczynski of the University of Maryland; E. Fenimore of Los Alamos National Laboratory; and D. C. Manchi of Argonne National Laboratories. Further information is contained in a TSP [see page 1].*
*GSC-14044*

## Power Supply for Miniature Quadrupole Mass Spectrometer

This lightweight, low-power system is designed to operate unattended for a long time.

*NASA's Jet Propulsion Laboratory, Pasadena, California*

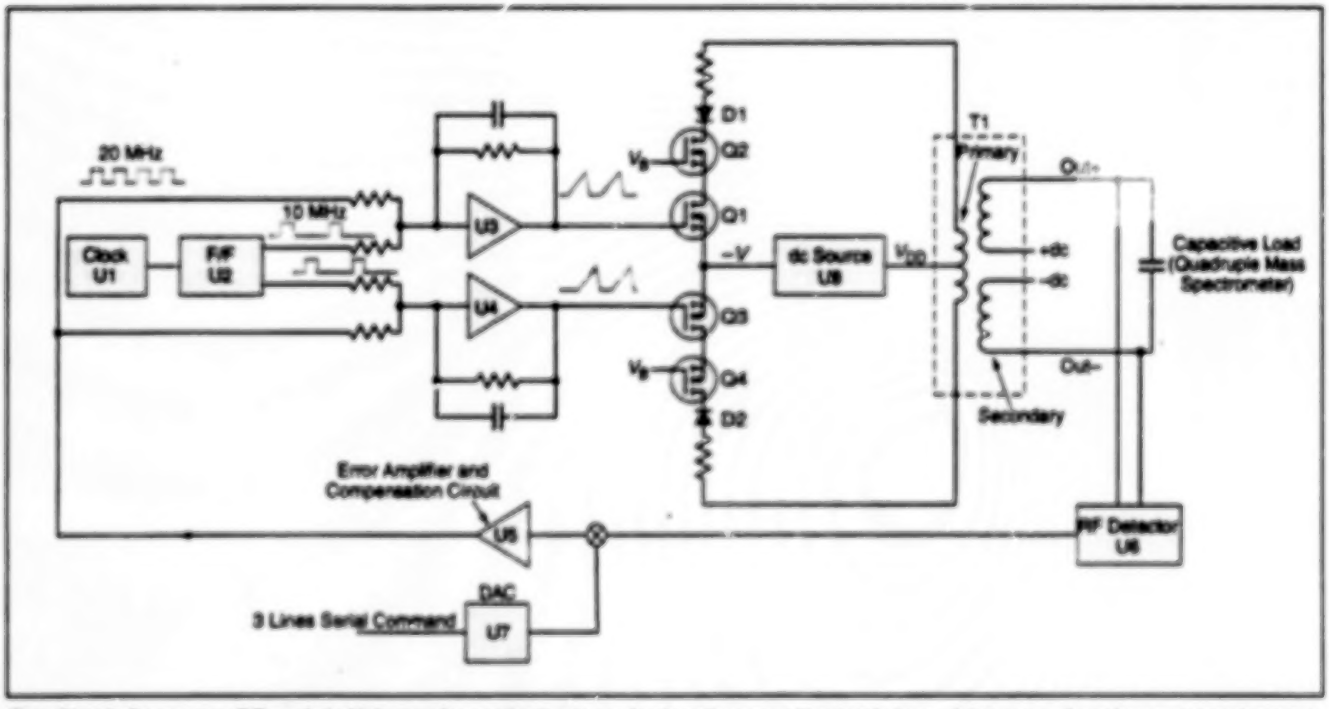


**This Circuit Generates RF and dc Voltages** for application to predominantly capacitive loads in a miniature quadrupole mass spectrometer.

A lightweight, low-power-consumption power supply has been developed to generate a combination of radio-frequency (RF) and dc voltages needed for the operation of a miniature quadrupole mass spectrometer that could operate unattended in the field for a long time, possibly using a battery as an energy source. More specifically, the circuit is designed to supply large, variable, frequency- and amplitude-stable RF voltages, variously floating or superimposed on positive or negative dc voltages, for application to primarily capacitive mass-spectrometer loads with capacitances of the order of 50 pF.

The figure is a simplified block diagram of an ac section of the power supply. This section puts out a signal with a frequency of 10 MHz, though in general, the frequency could be extended to as much as 100 MHz. The basic high-frequency clock signal for this section is generated by oscillator U1 at a frequency of 20 MHz. Flip-flop (FF) U2 divides the frequency by two, producing two 10-MHz pulse trains that differ in phase by a half cycle. Integrator and summing amplifiers U3 and U4 convert the 10-MHz clock pulses to sawtooth waveforms.

Q1 is a high-speed metal oxide/semiconductor field-effect transistor (MOSFET) that turns on when the sawtooth waveform applied to its gate goes beyond its threshold voltage. The conduction angle and the conducted current can be increased by increasing the sawtooth voltage. Q3 operates similarly to Q1, but a half cycle out of phase with Q1. Q1 and Q3 drive the primary windings of air-core transformer T1.

The air-core transformer design is chosen over a ferromagnetic-core design to obtain a desired combination of low weight, low loss, and low capacitance, and the ability to generate a large RF output voltage. The primary/secondary flux coupling, and thus the gain, can be adjusted in the design by choice of the winding ratio or can be changed by mechanical adjustment of the distance or overlap between the primary and secondary windings. These adjustments are inextricably coupled with the adjustment of the inductance of T1 to resonate with the capacitance of the affected portion of the quadrupole mass spectrometer.

U6 is an RF-detector circuit that generates a voltage proportional to the amplitude of the RF output signal. U5 is an error amplifier and compensation circuit, the output of which is a control signal proportional to the difference between (1) the actual RF output amplitude and (2) the commanded RF output amplitude as represented by the output of digital-to-analog converter U7. This control loop maintains a stable RF output amplitude during long-term operation.

One basic problem in the design of power-supply circuits like this one is to obtain a large dynamic range for the output signal. At a low level, the drive signal is coupled through the gate-to-drain capacitances of the MOSFETs, giving rise to an output signal much greater than the desired minimum. To counteract this effect and thereby extend the lower limit of the dynamic range of the mass spectrometer to below one atomic mass unit, a diode (D1) and a cascode stage (Q2 with bias $V_b$), is incorporated into the branch that contains Q1, and a similar combination (D2 and Q4) is added to the branch that contains Q3.

Another problem is obtaining sufficient sawtooth amplitude to drive the MOSFETs at the highest desired power levels; the peak amplitude (3 to 4 V) generated by currently available operational amplifiers is too low. In the present circuit, the return of the main dc source (U8) for driving the primary of T1 is referred to a negative voltage (–V). Thus, the apparent peak of the sawtooth signal applied to the MOSFET is increased by V, making it possible to reach correspondingly higher power levels.

*This work was done by Ara Chutjian, Dean Aalami, Murray Darrach, and Otto Orient of Caltech for* **NASA's Jet Propulsion Laboratory**. *Further information is contained in a TSP [see page 1].*

*In accordance with Public Law 96-517, the contractor has elected to retain title to this invention. Inquiries concerning rights for its commercial use should be addressed to*

*Technology Reporting Office*
*JPL*
*Mail Stop 122-116*
*4800 Oak Grove Drive*
*Pasadena, CA 91109*
*(818) 354-2240*

*Refer to NPO-20493, volume and number of this* NASA Tech Briefs *issue, and the page number.*

## RS-232-to-Infrared Transceiver

This unit can readily be reprogrammed for a different baud rate or protocol.

*Marshall Space Flight Center, Alabama*

A transceiver has been developed to serve as a data-communication link between (1) the RS-232-standard serial communication port of a personal computer (PC) running the Windows 95 or Windows NT operating system and (2) a remote infrared transceiver that is capable of operation at a baud rate ≤4 MHz. The PC-to-transceiver communication is 115.2 kilobits per second, while the infrared communication is at 4 megabits per second.

The transceiver includes a commercial off-the-shelf infrared transceiver module designed according to the Infrared Data Association (IrDA) standards, which were developed to promote compatibility among infrared networks for television receivers, computers, and other household devices. In the original application for which the transceiver was developed, there are requirements for small physical size and high flexibility of function for changing the PC baud rate and the sizes of transmitted data blocks. To satisfy these requirements, a programmable logic device (PLD) is included and is programmed with VHDL (very-high-speed integrated-circuit hardware description language).

One of the IrDA standard protocols dictates the use of a 16-bit header on each transmission, with consequent reduction of the effective data-throughput rate. However, the transceiver module is not operated according to this protocol; instead, to increase the data-throughput rate, a protocol that eliminates the 16-bit header was developed and is implemented in the PLD by use of VHDL.

The transceiver circuitry (see figure) consists of seven main subsystems:

1. *Voltage Regulator*
   This circuit converts 9-Vdc power from a wall transformer unit to 5-Vdc power used by the other subsystems.
2. *RS-232 Voltage-Level Converter*
   This circuit converts RS-232 transmitting (TxD) and receiving (RxD) ±10-Vdc logic levels to +5/0-Vdc logic levels used in the PLD.
3. *System Clock*
   The system clock operates at a frequency of 32 MHz (instead of 4 MHz) because 8× over-sampling of the 4-MHz received infrared signal is required for the

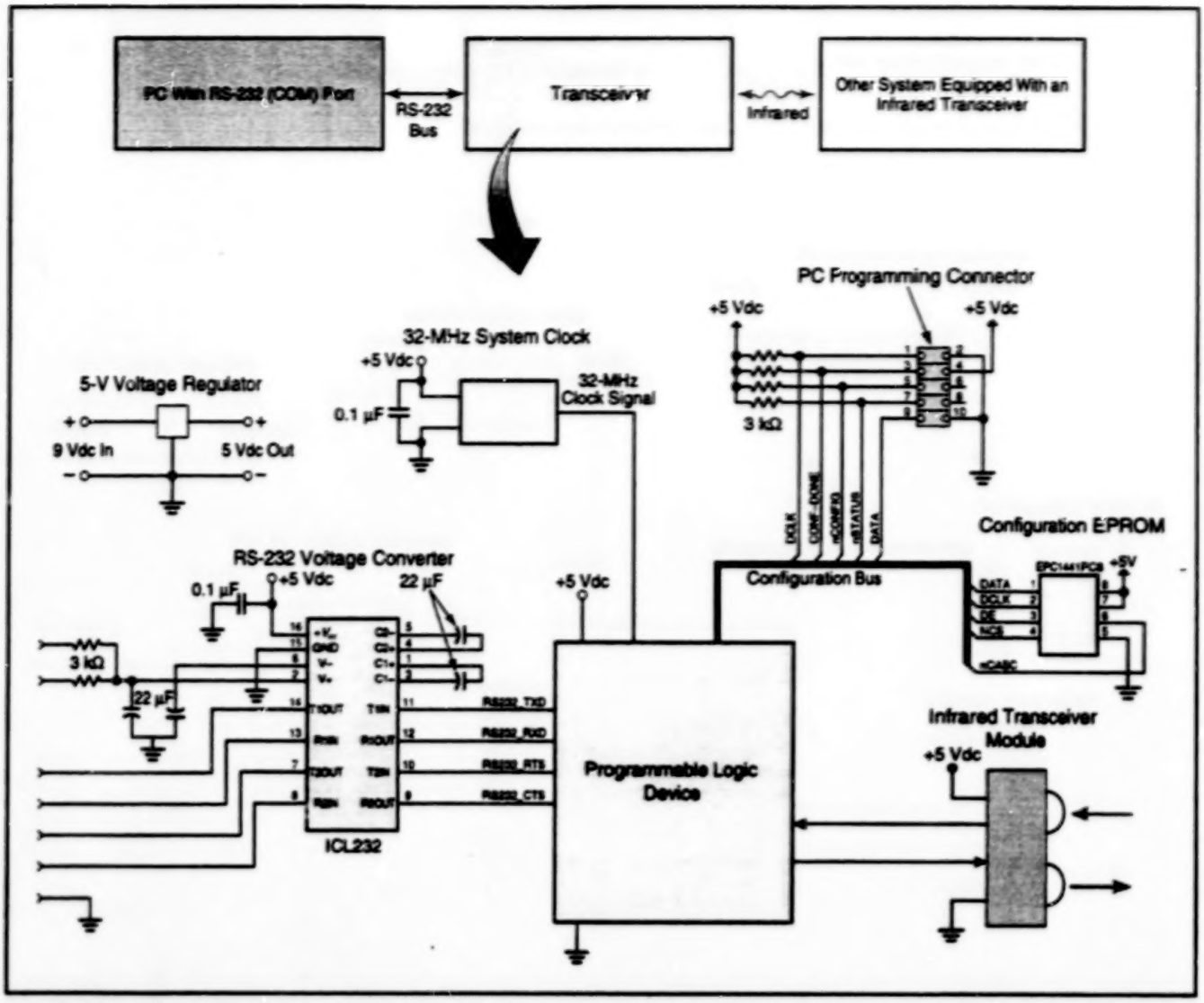


**The RS-232-to-Infrared Transceiver converts serial data streams between (a) a slower RS-232 electronic transmission medium and protocol and (b) a faster infrared transmission medium and protocol.**

4-MHz receiving logic in the PLD. The system clock also provides a master clock signal that is divided in frequency down to 921.6 kHz to enable 8× oversampling for the 115.2-kilobaud RS-232 receiving logic.

4. *Infrared Transceiver Module*
This module contains an infrared light-emitting diode (LED) and an optically gated transistor that operate at the same wavelength. Because it is an IrDA-standard module, it is compatible with commercial electronic devices.

5. *The PLD*
The PLD contains all the logic circuitry needed for conversion between an RS-232 data stream and a faster infrared data stream. Thus, most of the functionality of the transceiver is implemented in the PLD.

6. *Configuration EPROM*
The configuration erasable programmable read-only memory (EPROM) is used to reconfigure the logic in a the PLD, which logic is based on a static random-access memory (SRAM). Each time power is turned on, the PLD is configured with its hardware logic. Changes in the logic are implemented by changing or reprogramming the configuration EPROM.

7. *PC Programming Connector*
This is a socket for a cable connection to enable the use of a PC to program the PLD. This socket is used temporarily — during development — for configuring the PLD directly from a PC without reprogramming the EPROM.

*This work was done by Brandon Dewberry and Kosta Varnavas of* **Marshall Space Flight Center**.

*This invention is owned by NASA, and a patent application has been filed. For further information, contact Sammy Nabors, MSFC Commercialization Assistance Lead, at (256) 544-5226 or sammy.nabors@msfc.nasa.gov. Refer to MFS-31331.*

BLANK PAGE

# Electronic Systems

## Hardware, Techniques, and Processes


19 "Intelligent" Transceivers Would Predict Failures of Parts

20 Networks Based on Stack-Tree Topology and a 1394 Bus

21 Absolute Position Encoders Using Pattern Recognition

18

BLANK PAGE

# "Intelligent" Transceivers Would Predict Failures of Parts

Replacements could be ordered automatically to arrive just in time.

*NASA's Jet Propulsion Laboratory, Pasadena, California*

Special-purpose, "intelligent," computer-controlled, highly miniaturized radio transceivers have been proposed for use in monitoring critical and/or valuable pieces of equipment. These transceivers and associated electronic circuits would perform both diagnostic and prognostic monitoring functions: They would acquire and provide information on the history and current status of the monitored equipment. On the basis of this information, they would predict impending failures of components. Then they would order replacements for components expected to fail soon or for consumable supplies (e.g., fuel) expected to be exhausted soon; these orders would be submitted so that the needed replacements would arrive just in time.

The intelligent transceivers were conceived as means to relieve highly mobile military forces of much of the burden of maintenance and logistics. They could also prove useful in civilian industries in which it would be cost-effective to anticipate needs to replace components and/or replenish supplies; examples could include the automotive, vending-machine, and shipping industries.

Intelligent transceivers would have dimensions of no more than a few centimeters. They could be mass-produced relatively inexpensively by use of established integrated-circuit fabrication techniques. An intelligent transceiver would be connected with "smart-part" microchips that would be designed into major components and subassemblies of the equipment to be monitored (see figure). These microchips would contain sensors and sensor circuitry for monitoring the physical conditions and statuses of components and subassemblies. The sensors and circuits would be designed and calibrated to be especially sensitive to such failure-inducing phenomena as excessive wear, overstress, and temperature anomalies. The output signals from the smart chips would be collected by the transceiver and processed by algorithms that would predict times of probable failure of specific components.

An application-specific integrated circuit (ASIC) within the transceiver would provide the sensor-signal-processing algorithms and would serve as the interface between the rest of the transceiver and the smart sensor chips. During normal operation, the principal function of the ASIC would be to scan the sensors and perform continuous self-interrogation and diagnosis. Meanwhile, the time accumulating on each monitored component would be sent to a transceiver memory for continuous updating. During this operation, anomalies expected to lead to failures would be identified and times to failure would be estimated. The collected data would be processed into "plain-language" text with supplemental information derived from the memory, and requests for replacement of parts expected to fail would be transmitted — all automatically.

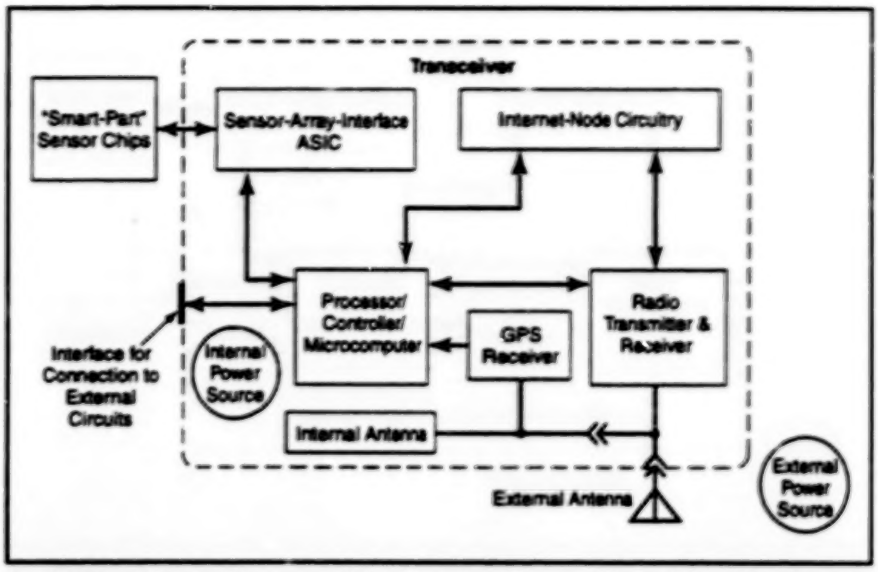


**An "Intelligent" Transceiver connected with "smart-part" sensor chips would provide information on the status of the equipment in which the sensor chips were embedded.**

Functions and characteristics of intelligent transceivers, in addition to those described above, would include the following:

- Each transceiver would contain a small battery or other power source and a small antenna for transmitting and receiving over a limited range; however, in normal operation, it would be connected, via a standardized receptacle, to a larger antenna and a power source in the monitored equipment to enable communication over a longer range.
- Although a transceiver would automatically signal the need for replacement of parts or other maintenance actions, it could also be interrogated manually for information on the status of the monitored equipment.
- Each transceiver would record the maintenance history of the monitored equipment.
- All components of the monitored equipment would be identified, in a transceiver memory, by part numbers.
- Instructions for repair and replacement would be contained in each transceiver memory and would be accessible via an infrared link to a display unit.
- Each transceiver would contain a Global Positioning System (GPS) receiver.
- Each transceiver would be capable of autonomously communicating with other transceivers to ascertain their locations.
- A transceiver on a damaged piece of equipment could interrogate other damaged pieces of equipment to determine what components could be salvaged and whether a replacement for a damaged component in its own damaged piece of equipment was locally available.
- Each transceiver would be capable of "learning" and updating its "knowledge" of the rates of wear of critical components.

*This work was done by Philip Moynihan and Govind Deshpande of Caltech for* **NASA's Jet Propulsion Laboratory.** *Further information is contained in a TSP [see page 1].*

*NPO-20699*

# Networks Based on Stack-Tree Topology and a 1394 Bus

COTS circuits can be configured to achieve high degrees of fault tolerance.

*NASA's Jet Propulsion Laboratory, Pasadena, California*

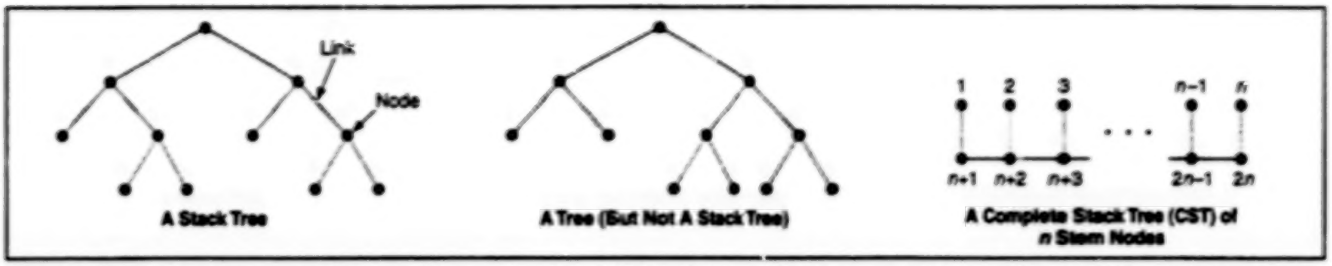


Figure 1. **Stack Trees** are constructed from three-port nodes. A leaf node is one that is connected to one other node denoted a stem node. Each stem node is connected to at most three other nodes, of which no more than two are stem nodes. A complete stack tree (CST) is one in which each stem node is connected to at least one leaf node.

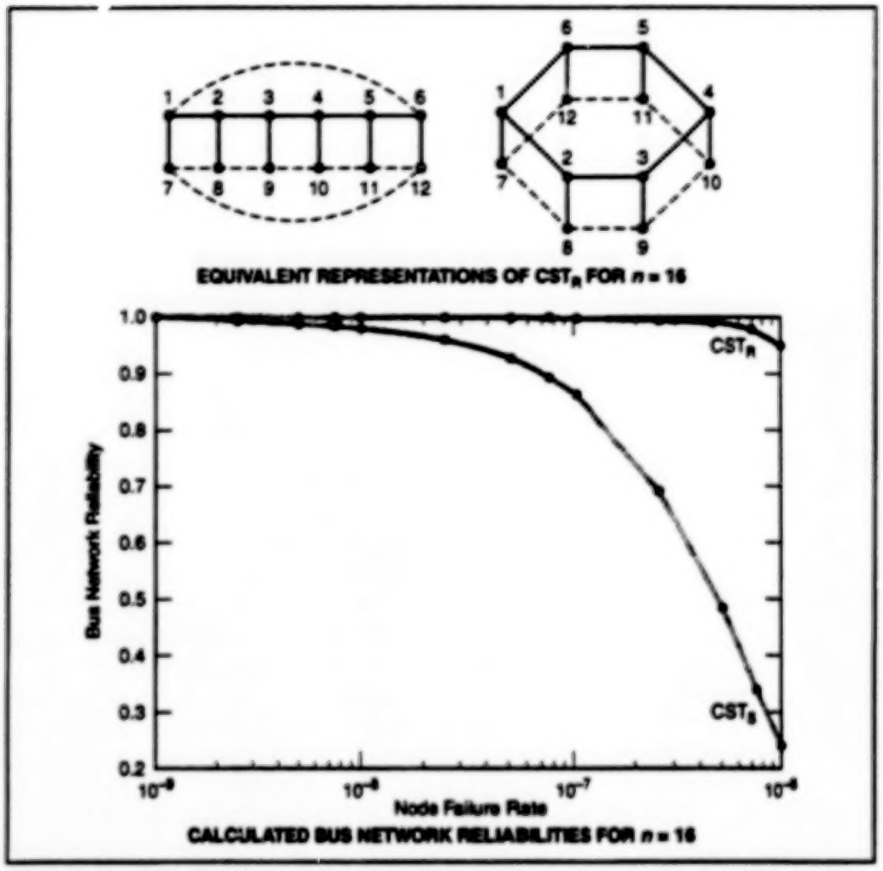


Figure 2. The **CST$_R$ Topology Is More Fault-Tolerant** than is the corresponding CST$_S$ topology. These curves were calculated for the example of a CST of $n = 16$ and an assumed fault-detection-and-reconfiguration coverage of 0.9999.

A method of designing fault-tolerant networks of computers and other electronic circuits has been conceived with a view toward minimizing costs by utilizing commercial off-the-shelf (COTS) products and standards for all system and component interfaces. The method involves, more specifically, utilization of selected features of the 1394 bus architecture and of the stack tree-topology (see Figure 1), which is a special case of the general tree topology and which complies with the 1394 standard. Of particular significance in the method is a specific type of stack tree denoted as Complete Stack Tree (CST) of $n$ stem nodes.

Taken by itself, the stack-tree topology is not fault tolerant: failure of any link partitions a stack tree into two segments, while failure of a stem node can partition the tree into two or three segments, depending on the specific design. Moreover, the 1394 standard does not permit loops, which would be formed if, for example, one were to connect the leaf nodes of a CST with spare links. However, the 1394 standard provides a "port disable" feature, which can be utilized to make any spare links "invisible" to the rest of the network. In the initial configuration of the network, the ports connected to the spare links are disabled, thereby disabling the spare links and preventing the formation of loops. In the event of failure of one or more nodes or a link of the initial network configuration, messages can be rerouted around the failed parts by enabling the appropriate ports to activate the appropriate spare links.

The upper part of Figure 2 schematically depicts a complete stack tree without spare links [denoted a "simplex complete stack tree" (CST$_S$)] and a complete stack tree with a spare link constructed to obtain a configuration called "CST$_R$" (where "R" refers to the fact that the resulting network topology is ring-like). The lower part of Figure 2 presents an example of calculated bus network reliabilities as functions of the node failure rate to demonstrate that a significant increase in reliability is expected to be achievable by the present method.

*This work was done by Leon Alkalai, Savio Chau, and Ann Tai of Caltech for* **NASA's Jet Propulsion Laboratory**. *Further information is contained in a TSP [see page 1].*

*In accordance with Public Law 96-517, the contractor has elected to retain title to this invention. Inquiries concerning rights for its commercial use should be addressed to*

*Technology Reporting Office*
*JPL*
*Mail Stop 122-116*
*4800 Oak Grove Drive*
*Pasadena, CA 91109*
*(818) 354-2240*

*Refer to NPO-20817, volume and number of this* NASA Tech Briefs *issue, and the page number.*

# Absolute Position Encoders Using Pattern Recognition

Advantages include longer travel at high resolution, low cost, and less sensitivity to damage.

*Goddard Space Flight Center, Greenbelt, Maryland*

Innovative optoelectronic encoders for measuring absolute, linear or angular position with super-high resolution have been invented. The new encoders rely on a combination of high-accuracy microlithography, optical projection, charge-coupled-device (CCD) array image detection, and image processing. Compared to conventional absolute encoders, the new encoders allow practically unlimited travel at exceptionally high resolution and are far less susceptible to scale damage or contamination.

Figure 1 is a block diagram of this type of encoder for measuring either linear position along an axis perpendicular to the page or rotary motion about a vertical axis in the page. The encoder includes a scale (as described below) that encodes linear or angular position and is attached to an object of interest which moves with respect to the remaining fixed parts of the encoder. The position encoding pattern on the scale comprises transparent marks on an opaque background such as clear areas in opaque chrome on a glass scale or a perforated metal tape. A printed pattern of light marks on a dark background could also be used in reflection.

A light source illuminates the scale from underneath in the figure, and a lens projects an image of the moving scale onto a CCD array in the camera head. The output of the CCD is processed though an analog-to-digital converter (ADC); the resulting digital image data are stored in an image memory. An image-data processing computer ("image processor" for short) analyzes the image data using pattern recognition algorithms, utilizing the known positions of the pixels in the image, to determine the absolute linear or rotary position of the scale pattern in the reference frame of the stationary parts of the encoder.

The upper part of Figure 2 shows an example of part of the pattern on a linear encoder scale (the pattern on a rotary scale is similar but fanned). In this case, the scale is for measuring position along a horizontal axis in the page. The pattern includes fiducials, smaller marks denoting code bits, and horizontal pattern registration marks. Together, a fiducial and its associated code bits and registration mark form a code group. The pattern of successive fiducials is strictly periodic in the direction of motion. The code bits in a code group uniquely identify each fiducial. The bit pattern could be chosen to represent any convenient

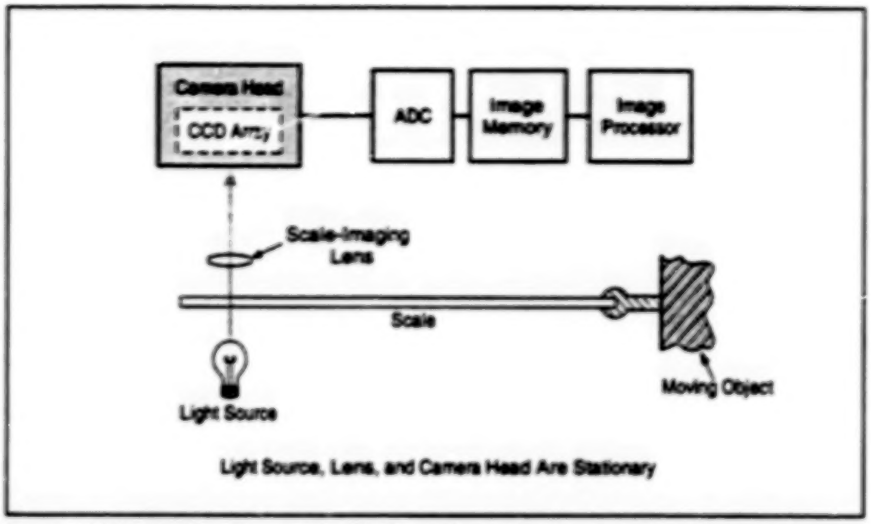


**Figure 1. Light Passing Through the Scale** attached to the moving object is focused to form an image of the scale pattern on the CCD. The remaining circuitry analyzes the pattern to determine the position of the object along the axis of motion, which is orthogonal to the page in this view.

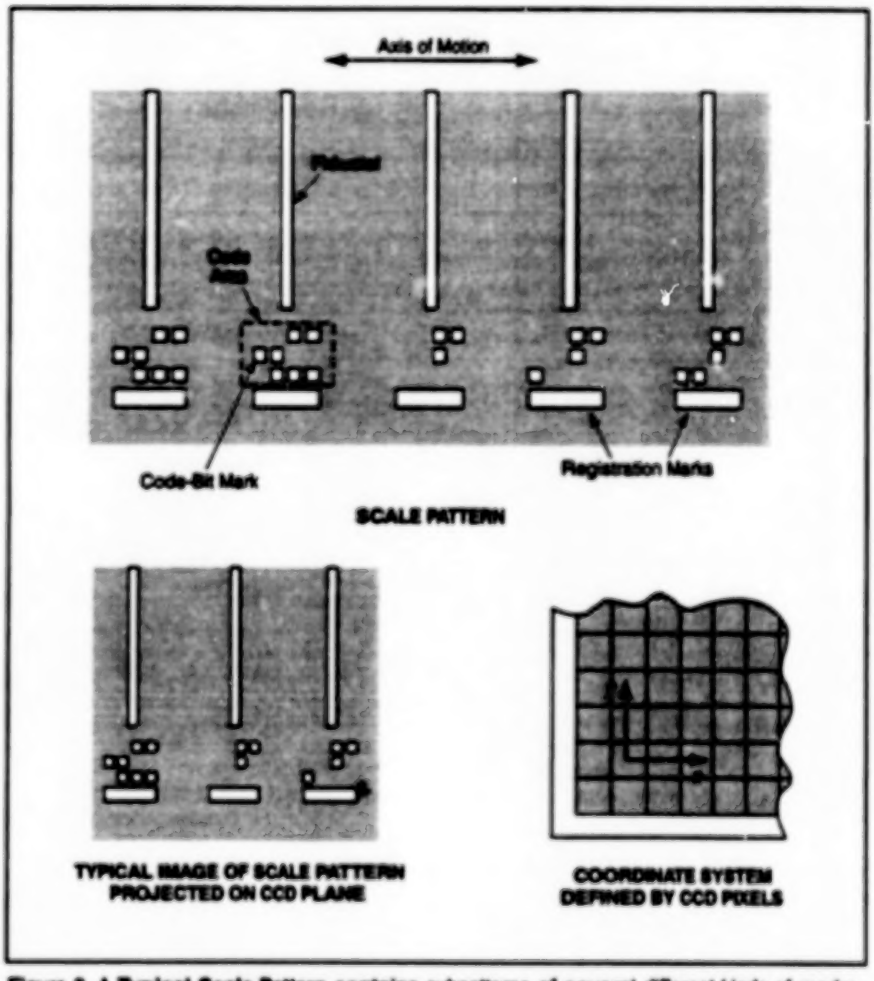


**Figure 2. A Typical Scale Pattern** contains subpatterns of several different kinds of marks. The marks provide information that the image processor uses to compute the absolute position of the scale to high resolution.

binary code; in this example, three rows of four bits each define a 12-position grid, so that each code group identifies one of $2^{12}$ or 4,096 fiducials.

The image processor utilizes the information in the image of the scale to determine the position of the scale along the axis of motion. For this purpose, one of the axes of the CCD array is aligned along the axis of motion so that the pixel pattern can readily be used as a reference frame. In effect, the binary codes themselves provide low-resolution, absolute position information by identifying which fiducial(s) is (are) imaged on the CCD at any particular time. The absolute position is determined to high resolution by finding the horizontal position of the image of each fiducial in the pixel coordinate frame. This could be done by any of such well-known image processing techniques as edge detection, peak detection, differentiation, or centroiding. However, because optically, the centroid of each fiducial image moves linearly across the CCD with scale motion, the preferred technique is centroiding; that is, computing the one dimensional centroid of the fiducial along the axis of motion in the pixel coordinate system.

For a given encoder geometry and CCD configuration, there is a scale pattern that is optimum in the sense that it yields the most reliable outcome with the highest sensitivity and accuracy with respect to true position. The use of a larger, more sophisticated CCD array enables the simultaneous acquisition of images of several code groups. Position data become more accurate if independent position determinations can be made for multiple code groups. It is desirable to select the scale pattern, optical magnification, and detector geometry to provide the images of at least two and sometimes three (depending on position) code groups on the CCD array. If more than one code group is in view at all times and if there are any variations in magnification, then those variations can easily be corrected because the true spacing of groups on the scale is known and the answer for each group must match as there is only one position being measured.

The arbitrary, multi-bit coding scheme makes it simple to extend the range of linear motion without sacrificing resolution. In a representative example, 12 code bits for fiducial bars spaced by 100 μm would make it possible to encode motion over a range of 409 mm with a sensitivity of 10 nm. A 15-bit pattern would, in principle, extend this range to nearly 3.3 m at the same resolution. A rotary version of the encoder with a 125-mm diameter code disk using 12 code bits has a sensitivity of about 0.02 arc-second. These parameters indicate both a sensitivity and a range considerably greater than prior encoders, even though the scale pattern is very much coarser. The coarser pattern can be manufactured at less cost with higher yield and makes the encoder less sensitive to damage of the scale. The fact that the encoder can produce a correct answer based on an image of a single fiducial also makes the encoder less sensitive to damage of the scale.

*This work was done by Douglas B. Leviton of* **Goddard Space Flight Center**. *Further information is contained in a TSP [see page 1].*

*This invention has been patented by NASA (U.S. Patent No. 5,965,879). Inquiries concerning nonexclusive or exclusive license for its commercial development should be addressed to the Patent Counsel, Goddard Space Flight Center [see page 1]. Refer to GSC-13703.*

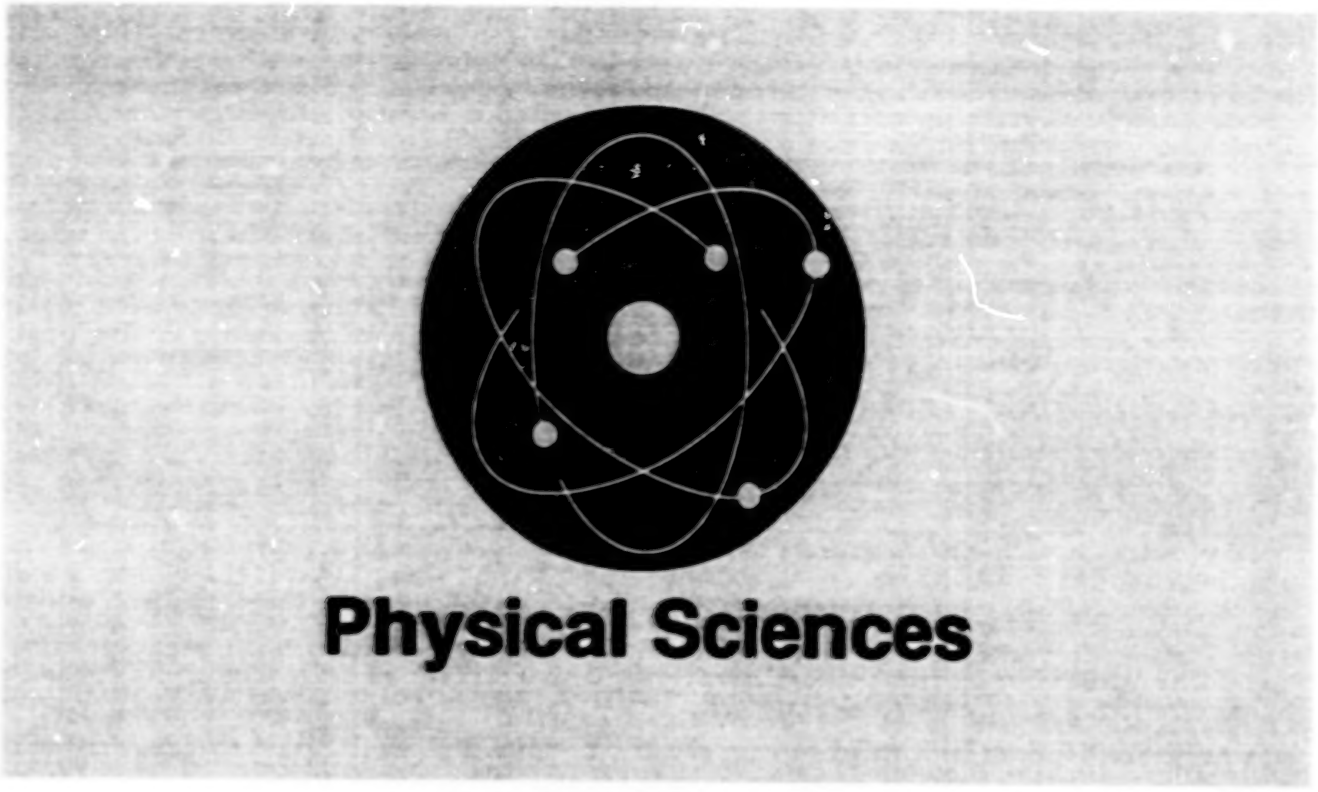

# Physical Sciences

## Hardware, Techniques, and Processes


25 Computer Program Automates Thermal Analyses
26 Controlling Crystal-Growth Habit in Directional Freezing
26 Vapor Corrosion Cell

BLANK PAGE

# Computer Program Automates Thermal Analyses

This program reduces the costs of thermal analyses of hypersonic flight systems.

*Lyndon B. Johnson Space Center, Houston, Texas*

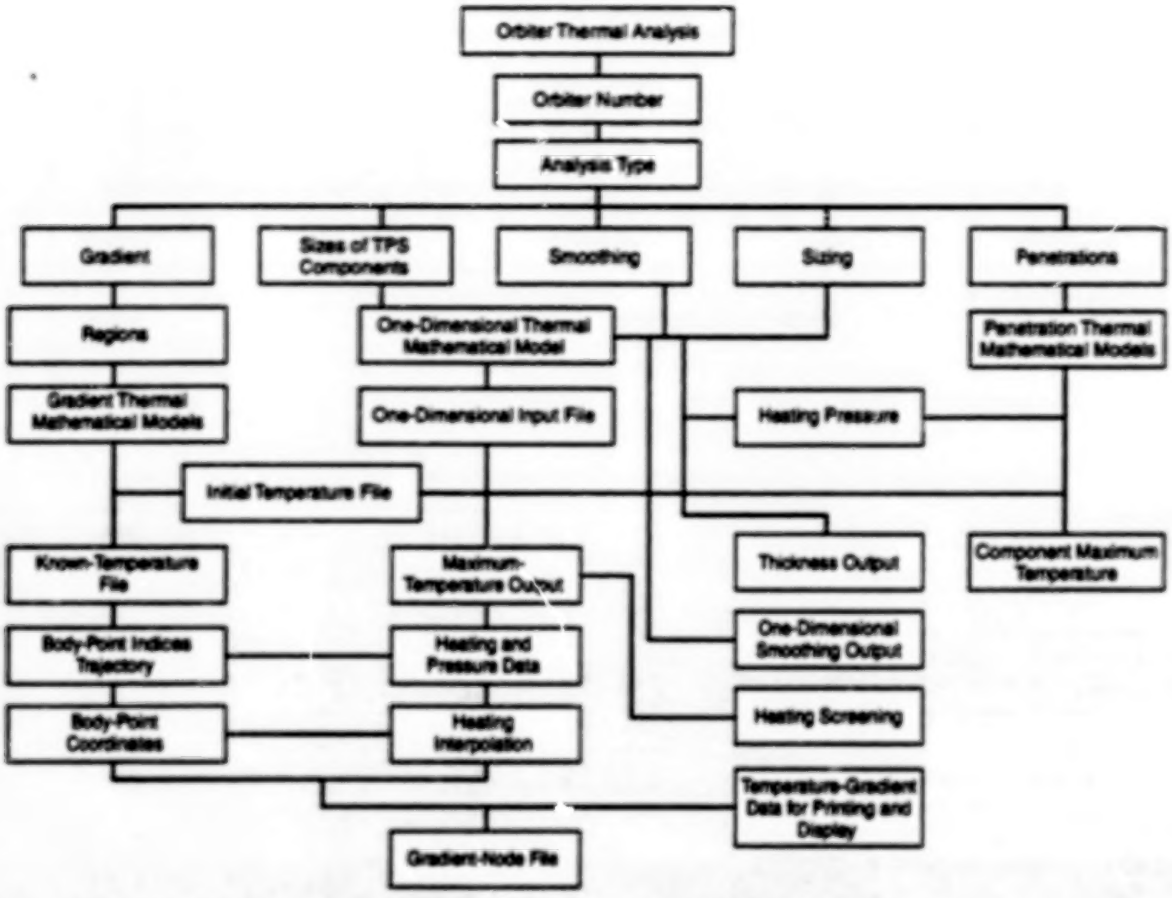


**This Program Flow Diagram has been made as concise as possible to show data links among data-base files.**

A computer program (see figure) has been developed to serve as a time- and cost-effective means of automating thermal analyses of such hypersonic flight systems as the space shuttle orbiter, the National Aerospace Plane (NASP), and the crew return vehicle (CRV). Heretofore, thermal analyses of the space shuttle orbiter have been performed manually and have, therefore, been hindered by long cycle times and the risk of human error. The present thermal-analysis automation program, which represents an advance in the state of the art, is expected to enable the sizing and analysis of thermal protection systems (TPSs) of re-entry space vehicles (RSVs) while increasing the accuracy of the analyses, reducing the amounts of labor needed to perform the analyses, and reducing the costs of the analyses.

Because the design of the TPS of a spacecraft affects the weight and thereby directly affects the operational cost and performance of the spacecraft, it is vital that adequate TPS materials be sized to minimum possible thicknesses. From a thermal perspective, the design is constrained by (1) the maximum temperature allowable on the spacecraft skin, and (2) the compositions of, and thermal gradients in, components of the TPS. Maximum thicknesses can be expected to differ, largely depending on locations on the spacecraft. To adequately define TPS thicknesses for an RSV, it is necessary to perform numerous TPS-sizing analyses. A sizing analysis is performed on a local-area basis, and engineering time is directly related to the number of sizing analyses performed. Moreover, coverage of spacecraft areas has sometimes been compromised to meet delivery schedules. Therefore, even after a sizing task has been completed, a considerable amount of engineering time is needed to verify the adequacy of faired TPS thicknesses, maximum skin temperatures, and structural thermal gradients.

With the help of the thermal-analysis automation program, these tasks can be performed easily — even if thermal analyses are required and must be repeated many times for spacecraft design. Additional capabilities of the program (e.g., those based on gradient smoothing techniques) enable preliminary airframe design to be performed to eliminate thermal-load problems in the early stages of spacecraft design. Heating-interpolation and heating-screening features can be applied to many different types and stages of thermal analysis. The trajectory difference can be evaluated easily by use of the heating-interpolation option of the program, and the heating-screening option helps to reduce the amount of work to a minimum by bypassing the thermal analysis in areas where changes in heating changes are negligible.

*This work was done by Sun I. Hong of Boeing North American for* **Johnson Space Center**. *Further information is contained in a TSP [see page 1].*
*MSC-22788*

## Controlling Crystal-Growth Habit in Directional Freezing

A method of controlling the crystal-growth habit in directional freezing has been devised. A substance can be purified by directional-freeze crystallization, wherein (1) the liquid phase of the substance is partially frozen, causing impurities to become preferentially concentrated in the remaining unfrozen liquid (they are more soluble in the liquid than in the solid), (2) the unfrozen liquid containing a large part of the impurities is extracted, and (3) the remaining crystalline phase is melted. The present method is directed toward reducing the entrapment of liquid within the crystalline structure, thus enhancing separation efficiency. The method is based on the observation that uniformity in heat-transfer conditions is of the utmost importance in forming uniform crystals in which little liquid is entrapped.

*This work was done by William M. Conlon of Polar Spring Corp. for* **Johnson Space Center**. *Further information is contained in a TSP [see page 1].*

*In accordance with Public Law 96-517, the contractor has elected to retain title to this invention. Inquiries concerning rights for its commercial use should be addressed to*

*Polar Spring Corp.*
*3501 Edison Way*
*Menlo Park, CA 94025*

*Refer to MSC-22518, volume and number of this NASA Tech Briefs issue, and the page number.*

## Vapor Corrosion Cell

This device detects corrosive gases that form during combustion and other processes.

*Lyndon B. Johnson Space Center, Houston, Texas*

The presence of corrosives in the Earth's atmosphere is of global concern. From acid rains that are destroying forests and disfiguring monuments like the Parthenon and the pyramids, to atmospheric pollutants that produce smog and induce emphysema in a significant number of people, the introduction of corrosives and other pollutants into the atmosphere is a critical and continuing environmental issue. No less critical to the space program is the presence of corrosives (reactive gases and water vapor) that are generated as byproducts of the launch process. The vapor corrosion cell developed for Johnson Space Center can be used to detect corrosives early in the formation process; that is, before significant quantities are vented into the atmosphere.

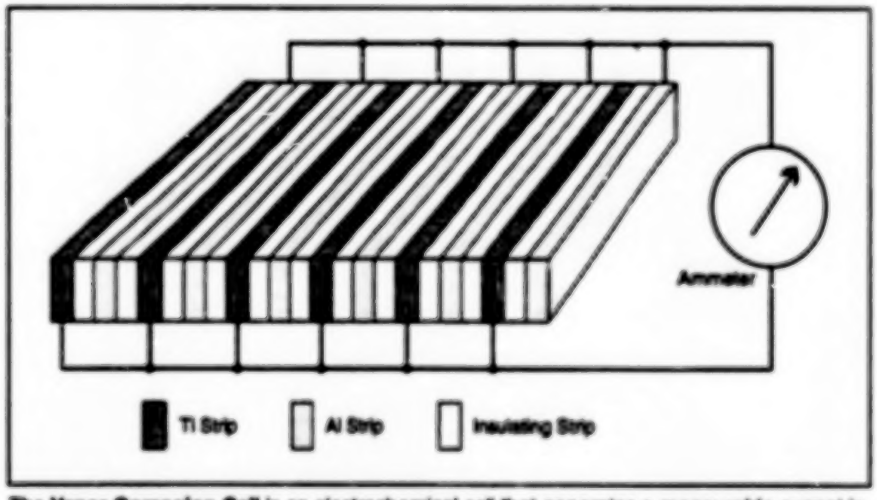


**The Vapor Corrosion Cell is an electrochemical cell that generates a measurable current in the presence of airborne corrosive substances.**

The development of the vapor corrosion cell went well beyond the original intent by leading to procedures that, if followed, are expected to help clean up the environment by severely limiting the harmful effects of such corrosive gases as nitrogen dioxide, hydrogen chloride, sulfur dioxide, and acidic aerosols. The availability of the vapor corrosion cell is also expected to encourage the testing and development of alloys that will prove resistant to corrosion. Moreover, by detecting corrosives at an early stage, the vapor corrosion cell can help to reduce costs, save time, and increase safety margins. This device is expected to be vital not only in the space program but also in the military, in activities and institutions that focus on the environment, in the aviation industry, and in any other industries, institutions, and activities in which there are risks that chemical processes will produce corrosive byproducts. Initial testing has shown that the vapor corrosion cell is highly sensitive to corrosives and that the cell can be reversed and rejuvenated to enable multiple measurements. Hence, the vapor corrosion cell is a significant step toward redressing the imbalance caused by the release of corrosives into the atmosphere through chemical processes.

In an atmosphere filled with chemically reactive gases and water vapor, such as are present at liftoff on a launch pad, the vapor corrosion cell is the only device capable of gauging the atmospheric corrosion potential. The cell (see figure) contains strips of alternating, dissimilar, electrically conductive materials — elemental metals or alloys — separated by thin strips of an electrically nonconductive material. In the example of the figure, the dissimilar electrically conductive materials are aluminum and titanium. This device is responsive to (1) the pressures of reactive vapors and the concentration of water vapor in the atmosphere; (2) the nature and surface areas of the two dissimilar conductors; (3) the nature and thickness of the electrically nonconductive separator; and (4) the ambient temperature. By controlling all but one of these parameters, one can operate the vapor corrosion cell in such a manner as to use it to measure the remaining parameters.

All the strips of each of the two electrically conductive materials are electrically connected in parallel. An electrochemical potential develops between the two dissimilar conductor strips when their edges are exposed to an atmosphere that contains water vapor and a reactive vapor or gas. If the electric circuit is closed, the current flows. The current can be measured as an indicator of electrochemical activity and corrosion on the exposed surfaces. The measured current can be taken to indicate presence of a hazardous gases, such as nitrogen dioxide,

hydrogen chloride, or sulfur dioxide, all of which, even in minute quantities, are corrosives capable of eating away at metals or polluting the atmosphere.

The vapor corrosion cell measures air pollutants and the corrosive effects of such pollutants on metal structures. It enables the development of criteria, based on resistance to corrosion, for better selection of materials. This device can be employed around launch platforms to perform real-time corrosion measurements and to provide data for predicting the life expectancies of metals exposed to corrosives. The device can also be used on aircraft platforms or ships to monitor the environment. At present, this device is used to address a major environmental concern — that of measuring corrosion caused by acid gases generated as byproducts of industrial chemical processes. This device thus becomes a new and valuable ally in the early detection of corrosives.

*This work was done by Dennis D. Davis and Anna H. DeArmond of AlliedSignal, Inc., for* **Johnson Space Center.**

*This invention is owned by NASA, and a patent application has been filed. Inquiries concerning nonexclusive or exclusive license for its commercial development should be addressed to the Patent Counsel, Johnson Space Center, (281) 483-0837. Refer to MSC-22871.*

BLANK PAGE

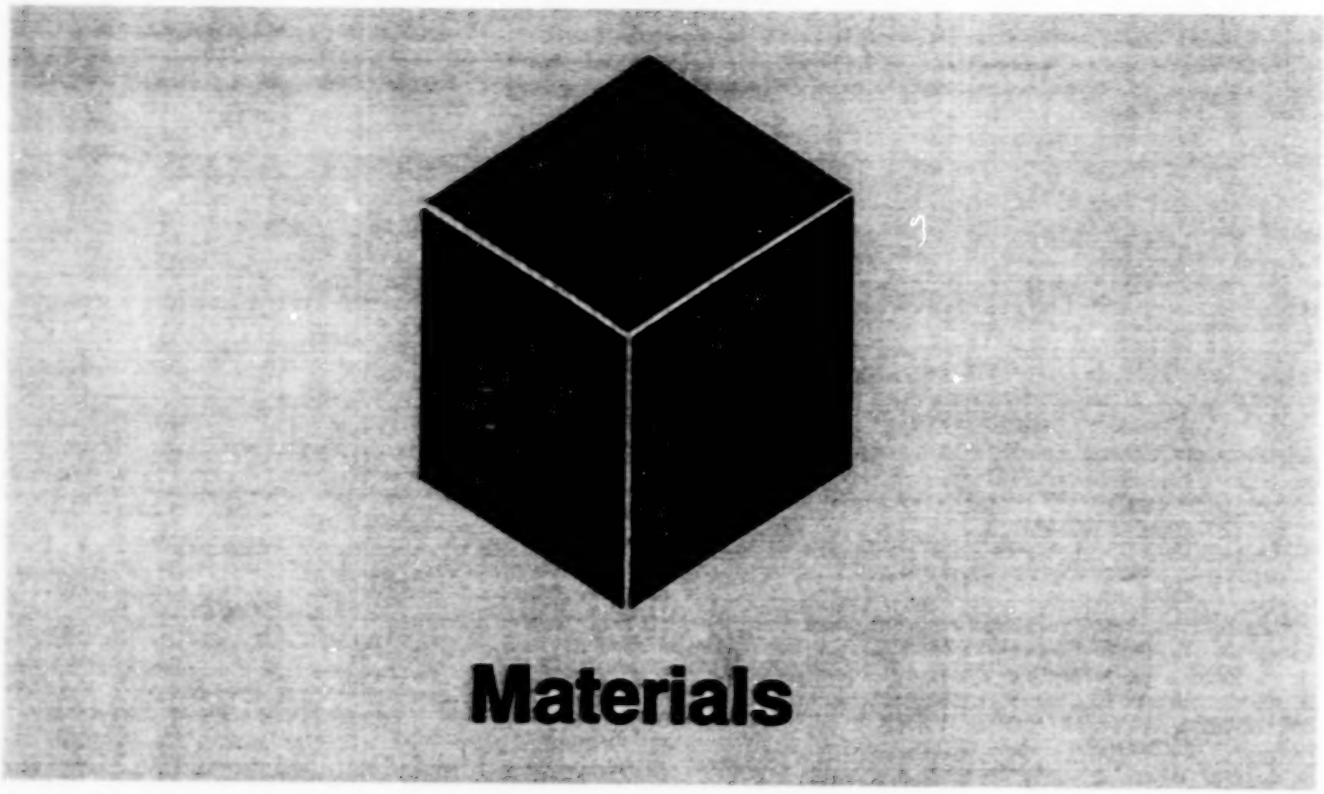

# Materials

## Hardware, Techniques, and Processes


31 Program Predicts Creep Lives of Ceramic Components
31 Using Commercial-Grade Tb/Dy in Magnetostrictive Actuators
32 Carbon Nanotubes as Anodes in Rechargeable Lithium-Ion Cells

BLANK PAGE

## Program Predicts Creep Lives of Ceramic Components

This software blends theoretical and empirical knowledge to predict creep rupture.

*John H. Glenn Research Center, Cleveland, Ohio*

Ceramics Analysis and Reliability Evaluation of Structures/Creep (CARES/CREEP) is a computer program that predicts the creep lives of ceramic structural components. [CARES/CREEP should not be confused with the related program CARES/LIFE, which was described in "Program for Evaluation of Reliability of Ceramic Parts," *NASA Tech Briefs*, Vol. 20, No. 3 (March 1996), page 28.] CARES/CREEP is integrated with the commercially available ANSYS finite-element code and is intended to be used, in conjunction with ANSYS, to design ceramic structural components of advanced turbine engines.

The need to predict creep lives for hot engine structures arises from the expected service conditions and durability requirements. The high-temperature properties of ceramic structural components make them attractive for use in advanced turbine engines, the design operational lives of which can exceed 10,000 hours. In order to enable ceramic components to last such long times, one must subject them to relatively low stresses. The combination of high temperatures and low stresses typically causes failures of monolithic ceramic components to occur in the creep regime.

CARES/CREEP utilizes the finite-element heat-transfer and nonlinear-stress-analysis capabilities of ANSYS to obtain temperature and stress distributions in a ceramic component. CARES/CREEP takes account of time-varying creep-strain distributions (stress relaxation). The creep life of a component is discretized into short time steps, during each of which the stress and strain distributions are assumed constant. The increment of damage at each time step is calculated on the basis of a modified Monkman-Grant creep-rupture criterion. The cumulative damage is subsequently calculated as time elapses in a manner similar to that of Miner's rule for cyclic fatigue loading. Failure is assumed to occur when the normalized cumulative damage at any point in the component reaches unity. The elapsed time to occurrence of such a failure is considered to be the creep rupture life of the component.

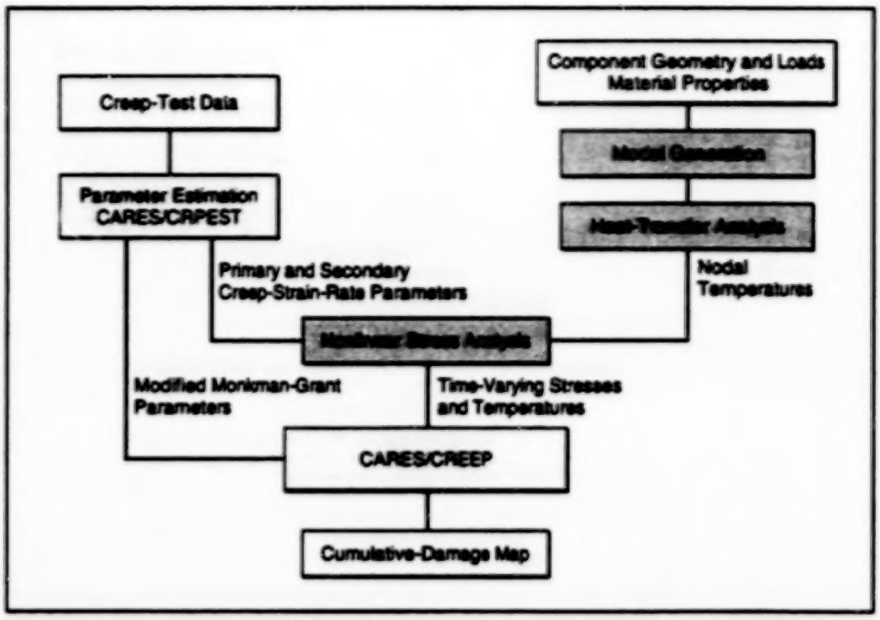


**This Block Diagram** depicts the flow of information in a creep analysis of a monolithic ceramic component by use of CARES/CREEP.

CARES/CREEP is run as a postprocessor of ANSYS output. The program (see figure) consists of two modules: The first module is a parameter-estimation subprogram that computes (1) the primary creep parameters based on the time hardening rule (a widely accepted constitutive equation that closely approximates empirical data on creep as a function of stress, temperature, and time), (2) the steady-state parameters based on the Norton equation, and (3) the creep-rupture parameters based on the modified Monkman-Grant criterion. The second module calculates the cumulative damage and thus the creep-rupture life of the component in question. Among the outputs of the program is a cumulative-damage plot for graphical rendering of critical regions of the component.

*This work was done by John P. Gyekenyesi of* **Glenn Research Center**, *Lynn M. Powers of Cleveland State University, and Osama M. Jadaan of the University of Wisconsin. Further information is contained in a TSP [see page 1].*

*Inquiries concerning rights for the commercial use of this invention should be addressed to NASA Glenn Research Center, Commercial Technology Office, Attn: Steve Fedor, Mail Stop 4–8, 21000 Brookpark Road, Cleveland, Ohio 44135. Refer to LEW-16917.*

## Using Commercial-Grade Tb/Dy in Magnetostrictive Actuators

This material would offer performance and cost advantages over purer material.

*NASA's Jet Propulsion Laboratory, Pasadena, California*

Single crystals of Tb-Dy alloys exhibit magnetostrictive strains approaching 1 percent and can generate forces sufficiently large to make them useful as actuators in cryogenic mechanical devices. These actuators offer many advantages over piezoelectric actuators and actuators using motion feedthroughs from higher temperature. Unfortunately, the preparation of single crystals of Tb-Dy alloys is difficult and costly, and will likely remain so. The limited availability of single crystals could impede the development of this new actuator technology. Since polycrystals are much simpler to prepare and are less costly, textured polycrystalline materials are being developed as alternatives to single crystals, as discussed in "Polycrystalline Tb/Dy Alloy for Magnetostrictive Actuators" (NPO-20273) *NASA Tech Briefs*, Vol. 23, No. 8, (August 1999) page 44. Continued efforts to reduce

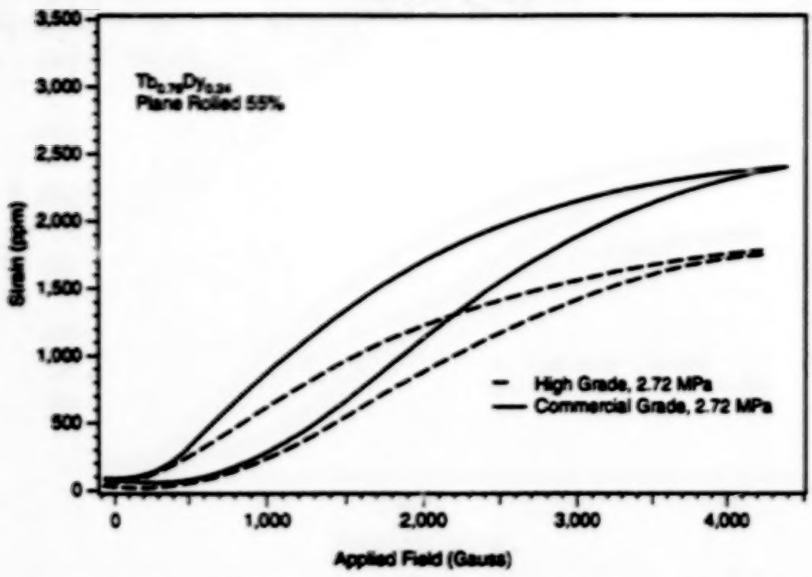


**Strain Versus Applied Field** is shown for commercial-grade and high-purity polycrystalline Tb-Dy.

the cost of magnetostrictive polycrystals have led to the use of lower cost commercial grade (total purity 99.7 percent) Tb-Dy material [as opposed to expensive high-purity (99.94 percent) material required for the growth of single crystals].

In general, a material containing many individual crystals with random orientation will not have a large bulk magnetostriction. Crystallographic texture describes the average orientation of the individual crystallites in the material. It is possible to achieve a preferred texture by various materials-processing methods, but one of the simplest is deformation processing. The Tb-Dy alloy was arc-melted and drop-cast into a chilled copper mold. Since the as-cast ingot shows strong crystallographic texture, the material was first cold rolled to a 35-percent reduction in thickness and heat treated for 1.5 h at 950 °C to induce recrystallization. This step was intended to provide a random initial orientation of spherical grains, although our bulk thermal expansion measurements indicate that significant texture remained after this step. The specimen was then plane-rolled by 55 percent and annealed at 350 °C to relieve strain. This rolling and annealing combination was performed once or repeated a number of times. It can be seen in the figure that the commercial specimen exhibits 2,400 ppm magnetostriction, while the high-purity specimen exhibits only 1,750 ppm magnetostriction. It may be that the additional impurities in the commercial-grade material limits grain boundary growth during heat treatments, and studies are currently underway to relate grain size and texture to magnetostriction. Although impurities that inhibit grain growth are detrimental to the fabrication of single-crystal materials, these impurities may not be a problem for polycrystalline materials. The use of Tb and Dy of lower purity may be an important practical advantage of polycrystalline materials, since the lower purity materials can be obtained at significantly lower cost and with greater reliability.

*This work was done by Jennifer Dooley and Brent Fultz of Caltech for* **NASA's Jet Propulsion Laboratory**. *Further information is contained in a TSP [see page 1].*

*In accordance with Public Law 96-517, the contractor has elected to retain title to this invention. Inquiries concerning rights for its commercial use should be addressed to*

*Technology Reporting Office*
*JPL*
*Mail Stop 122-116*
*4800 Oak Grove Drive*
*Pasadena, CA 91109*
*(818) 354-2240*

*Refer to NPO-20697, volume and number of this* NASA Tech Briefs *issue, and the page number.*

## Carbon Nanotubes as Anodes in Rechargeable Lithium-Ion Cells

The discharge capacities of these nanotubes exceed those of other forms of carbon.

*John H. Glenn Research Center, Cleveland, Ohio*

Carbon nanotubes (also known as "bucky tubes") have shown promise for use as anode materials in rechargeable lithium-ion power cells. In comparison with graphite and other forms of carbon used under identical conditions, bucky tubes exhibit greater specific discharge capacity and greater specific energy; this increase has been attributed to the greater electronegativity of bucky tubes and the consequent ability of bucky tubes to accommodate more lithium ions per unit of carbon. The success achieved thus far in the development of bucky-tube anodes with high reversible (charge/discharge) lithium-ion capacities is a result of advances in (1) the production of single- and multi-walled bucky tubes by both arc and non-arc techniques, (2) techniques for purification, (3) techniques for opening the ends of the tubes to admit lithium ions for intercalation, and (4) techniques for fabricating electrodes from bucky tubes.

A recent experimental investigation undertaken as part of this development emphasized the electrochemical performances of open-ended single- and multi-wall bucky-tube anodes in half-cell tests. (In practical full cells, bucky tubes as anode materials would be used in conjunction with $LiNiO_2$, $LiMnO_2$, or $LiCoO_2$ as cathode materials.) In the tests, anodes made from open-ended single-wall bucky tubes exhibited specific discharge capacities as high as 640 mAh/g, and anodes made from open-ended multi-wall bucky tubes exhibited discharge capacities of about 385 mAh/g. In contrast, the theoretical limit of capacity of graphite is only 372 mAh/g.

*This work was done by R. O. Loutfy, S. Hossain, and M. Y. Saleh of Materials and Electrochemical Research Corp. for* **Glenn Research Center**. *Further information is contained in a TSP [see page 1].*

*Inquiries concerning rights for the commercial use of this invention should be addressed to NASA Glenn Research Center, Commercial Technology Office, Attn: Steve Fedor, Mail Stop 4–8, 21000 Brookpark Road, Cleveland, Ohio 44135. Refer to LEW-16727.*

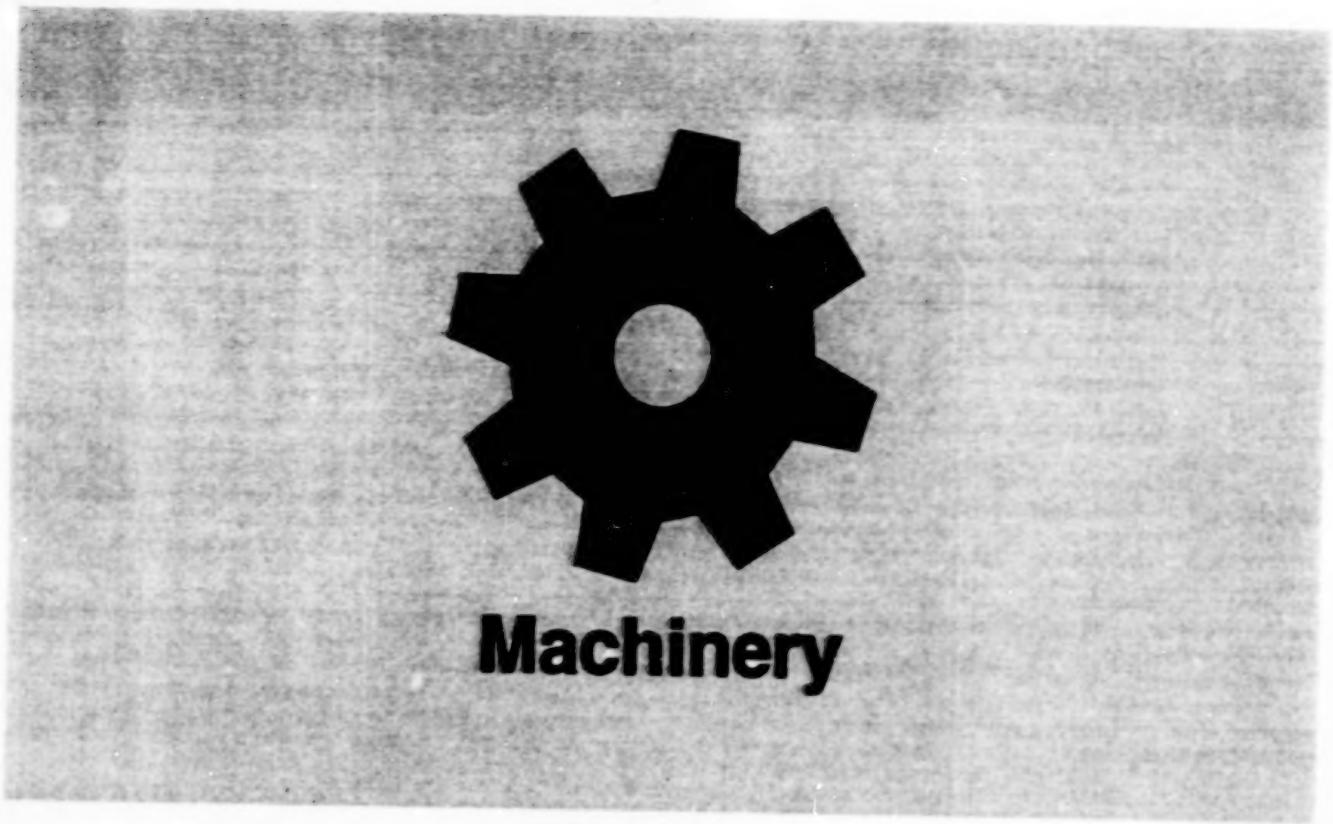


## Hardware, Techniques, and Processes

35 Comprehensive Micromechanics-Analysis Code (MAC/GMC)
35 Pulse-Mode Reaction Control System Thruster

BLANK PAGE

## Comprehensive Micromechanics-Analysis Code (MAC/GMC)

Composite-material structures with complex thermomechanical load histories can be analyzed.

*John H. Glenn Research Center, Cleveland, Ohio*

Micromechanics Analysis Code With Generalized Method of Cells (MAC/GMC) is a comprehensive, user-friendly, efficient computer program that predicts the elastic and inelastic thermomechanical responses of continuous and discontinuous composite materials with arbitrary internal microstructures and reinforcement shapes. This program enables the efficient analysis of composite structures subjected to complex thermomechanical load histories. MAC/GMC won second place in the 1997 NASA Software of the Year competition and has been applied in industrial, government, and academic settings to such diverse composite-material structures as turbine parts, tires, and even brain tissues.

The predictive capability of MAC/GMC rests on the mathematical model known as the generalized method of cells (GMC) — a continuum-based model of micromechanics that provides closed-form expressions for the macroscopic response of a composite material in terms of the properties, sizes, shapes, and responses of the individual constituents or phases that make up the material. The viscoplastic and fatigue-life characteristics of the constituents or phases, are in turn, represented by advanced, physics-based mathematical submodels.

The GMC also incorporates expressions that relate stress and strain fields within individual constituents to macroscopically applied stresses and strains via stress-concentration factors. These expressions make possible the investigation of failure processes at the microscopic level at each step of applied-load history. The GMC also affords a capability for studying the influence of the strengths of bonds of fiber/matrix interfaces; this is an important capability because the strengths of these bonds strongly influence the progression of damage.

MAC/GMC enhances the basic capabilities of the GMC by providing a modular software framework wherein one can take advantage of any or all of the following options:

- Various thermal, mechanical (stress or strain), and thermomechanical load histories can be imposed.
- Different integration algorithms can be selected.
- Any of a variety of constitutive submodels for constituent materials can be selected from a library of such models or implemented via a subroutine defined by the user.
- Any of a variety of fiber architectures (unidirectional, laminate, and woven) can be selected from a library of representative volume elements or be defined by user.
- A postprocessing subprogram for graphical display of microscopic and macroscopic field quantities is available (MACPOST).

The most outstanding feature of MAC/GMC is its ability to accurately model composites with laminated and woven fiber architectures at minimal cost and with minimal input by the user. MAC/GMC can be executed in conjunction with standard linear and nonlinear finite-element analysis programs for cost-effective design and analysis of large structures, including fully time-dependent deformation behavior of constituents. It is also possible to model porosity, damage, interfacial regions around inclusions, and deterioration of interfaces. Multiaxial states of stress or strain can be applied and predicted accurately, regardless of the orientations of fibers.

One advantage of the use of constitutive submodels is that any type of simple or combined loading (e.g., multiaxial stress) can be applied, irrespective of symmetry or asymmetry, and without resorting to different boundary-condition application strategies. An analytical macro elastic-thermo-inelastic constitutive law offers the advantage of reducing the amount of memory needed in a finite-element structural-analysis code; it also enables coupling of optimization algorithms with the solution for automated tailoring of the material and structure under analysis. Furthermore, this formulation has been shown to predict macroscopic behavior accurately, given only a few subcells within a repeating cell.

*This work was done by Steven M. Arnold of* **Glenn Research Center**, *Brett A. Bednarcyk of Ohio Aerospace Institute, and Thomas E. Wilt and Daniel E. Trowbridge of the University of Akron. Further information is contained in a TSP [see page 1].*

*Inquiries concerning rights for the commercial use of this invention should be addressed to NASA Glenn Research Center, Commercial Technology Office, Attn: Steve Fedor, Mail Stop 4–8, 21000 Brookpark Road, Cleveland, Ohio 44135. Refer to LEW-16870.*

## Pulse-Mode Reaction Control System Thruster

This thruster burns nontoxic propellants.

*Lyndon B. Johnson Space Center, Houston, Texas*

A spacecraft reaction-control-system (RCS) thruster now undergoing development generates a thrust of 870 lbf (3,870 N) by burning ethanol and liquid oxygen (LOX), which are nontoxic. The performance of the thruster has been tested in operation in multiple pulse modes with pulses as short as 160 ms; such pulses are typical of those required for the space-shuttle RCS.

This test is the first successful demonstration of a liquid/liquid-fed thruster in pulse-mode operation. The use of thrusters fed by nontoxic liquids is expected to afford great benefits — not only in space-shuttle operations but also in the operations of reusable first-stage or liquid-fueled fly-back boosters or, indeed, of any reusable launch vehicle currently produced by NASA or the Department of Defense.

Today, the market for thrusters like this one is limited to the second-stage RCS and orbital maneuvering system of the Kistler K-1 vehicle (a commercial reusable launch vehicle), to the RCS of the VentureStar reusable launch vehicle, and to upper-stage RCSs in general; however, with the increase in the number of commercial aerospace companies launching unmanned rockets, the technological advances made in the development of this thruster can be expected to affect the commercial field significantly. For NASA, the use of LOX and ethanol in the shuttle RCS thrusters will not only increase safety but will also reduce costs.

*This work was done by Paul Philipsen, Lee May, and Ross Hewitt of GenCorp for* **Johnson Space Center**.
*MSC-23017*

BLANK PAGE

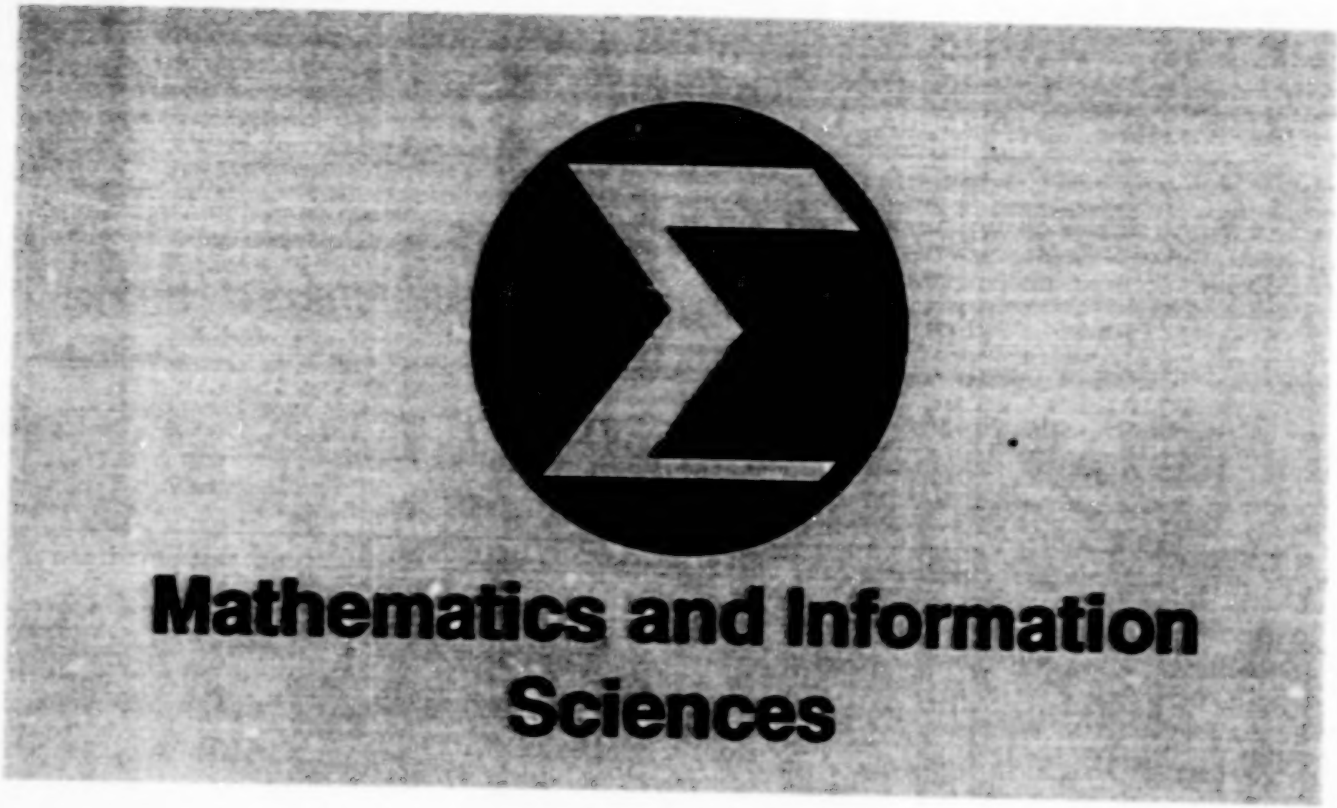


## Hardware, Techniques, and Processes

39 Software for Analyzing Forth Programs
40 Rule-Based "Intelligent" Monitoring Software
41 Automated Generation of Acoustic-Propagation Computer Codes

BLANK PAGE

# Software for Analyzing Forth Programs

Various parts of code can be categorized and quantified in selectable ways.

*Marshall Space Flight Center, Alabama*

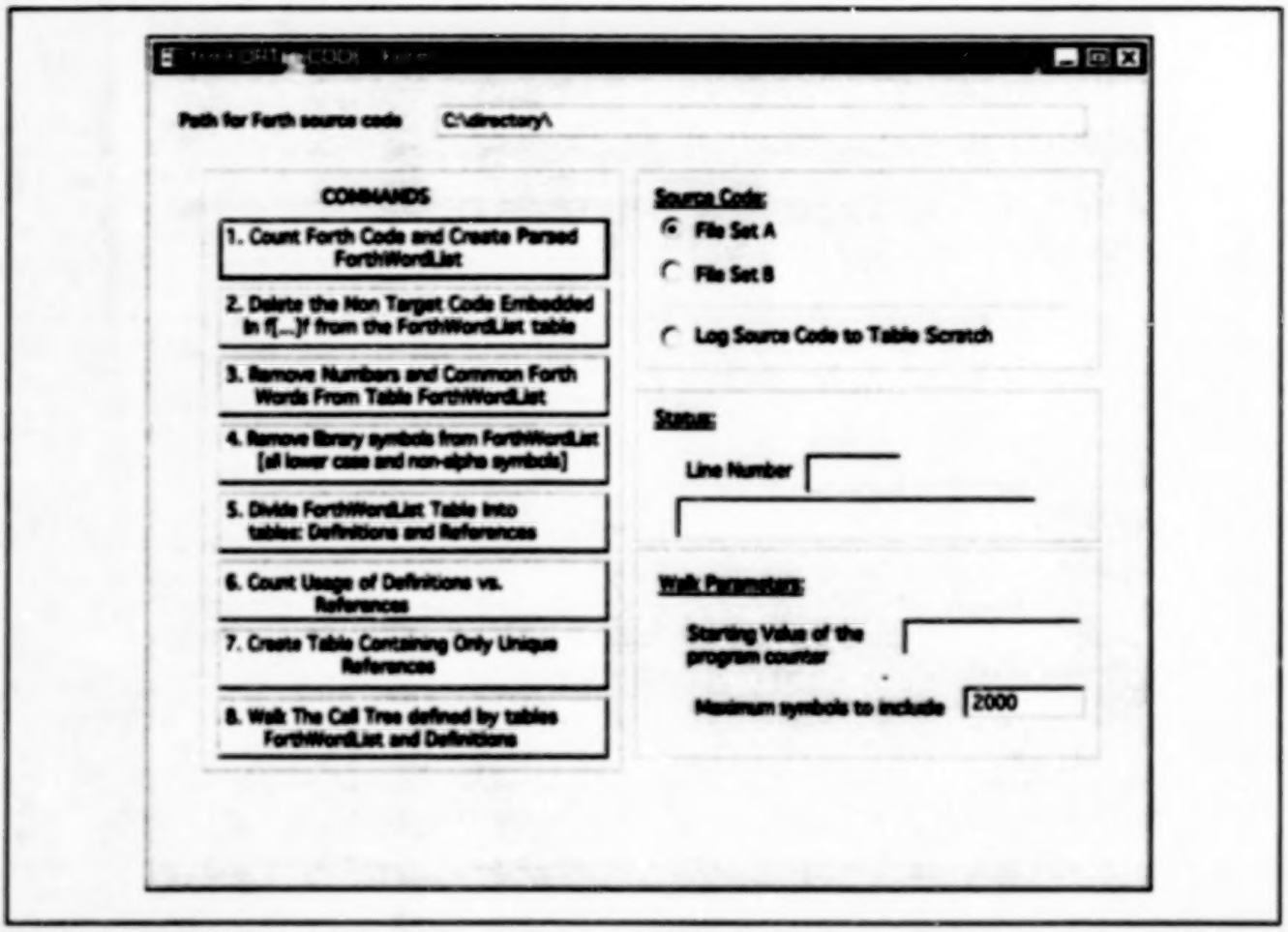
Path for Forth source code
C:\directory\
COMMANDS
1. Count Forth Code and Create Parsed ForthWordList
2. Delete the Non Target Code Embedded in f[...]f from the ForthWordList table
3. Remove Numbers and Common Forth Words From Table ForthWordList
4. Remove library symbols from ForthWordList [all lower case and non-alpha symbols]
5. Divide ForthWordList Table Into tables: Definitions and References
6. Count Usage of Definitions vs. References
7. Create Table Containing Only Unique References
8. Walk The Call Tree defined by tables ForthWordList and Definitions
Source Code:
File Set A
File Set B
Log Source Code to Table Scratch
Status:
Line Number
Walk Parameters:
Starting Value of the program counter
Maximum symbols to include
2000

**The Main Form of FSCATS is an interactive display containing command buttons for selecting among options for processing code and obtaining the results of processing.**

Forth Source Code Analysis Tool Set (FSCATS) is a computer program that provides a wide range of capabilities for documenting, analyzing, and reverse-engineering computer programs written in the Forth programming language. FSCATS also aids in the management of software, estimating costs of software, and development of metrics for characterizing software.

The functions performed by FSCATS include the following:

- Categorizing lines of code and counting the lines in each category;
- Producing cross-references for all words, constants, and variables;
- Producing cross-references for all definitions;
- Identifying unused and multiplicate definitions;
- Identifying unused and undefined Forth words; and
- Identifying development system code, missing library definitions, and missing compiler definitions; and
- Listing a call tree at selectable levels of detail
  — All symbols (full structure)
  —Selected categories of symbols (partial structure)
  —Only application-code-type symbols (classical structure chart).

The aforementioned functions are enhanced by presenting all results in tables in the Microsoft Access software environment. The availability of results in tabular form provides the user with extraordinary flexibility in tailoring FSCATS to produce a wide range of sorted and filtered views. By use of the report capabilities of Microsoft Access, tables of summary information can readily be printed as needed.

The figure depicts an interactive display, denoted the "main form," used to control the operation of FSCATS. The main form contains eight command buttons for processing a source code and obtaining results. Command buttons 2, 3, and 4 enable the user to view the source code at the three levels of detail mentioned above. The structure-chart level obtains when all filters are used and the remaining code set consists of application-level Forth words.

FSCATS was written for execution on an IBM-compatible computer containing a '486 or higher processor with at least 10MB of free hard-disk space and 16MB of random-access memory. The Windows 95 or Windows NT operating system, the Office 95 software, and Microsoft Access (version 7.0 or later) are needed to run FSCATS.

*This work was done by Michael Neighbors of Micro Craft Inc. for* **Marshall Space Flight Center**. *For further information, please contact the company by e-mail at theneighbors@zebra.net.*
*MFS-31255*

# Rule-Based "Intelligent" Monitoring Software

This program helps to automate the analysis of batch or real-time data.

*Dryden Flight Research Center, Edwards, California*

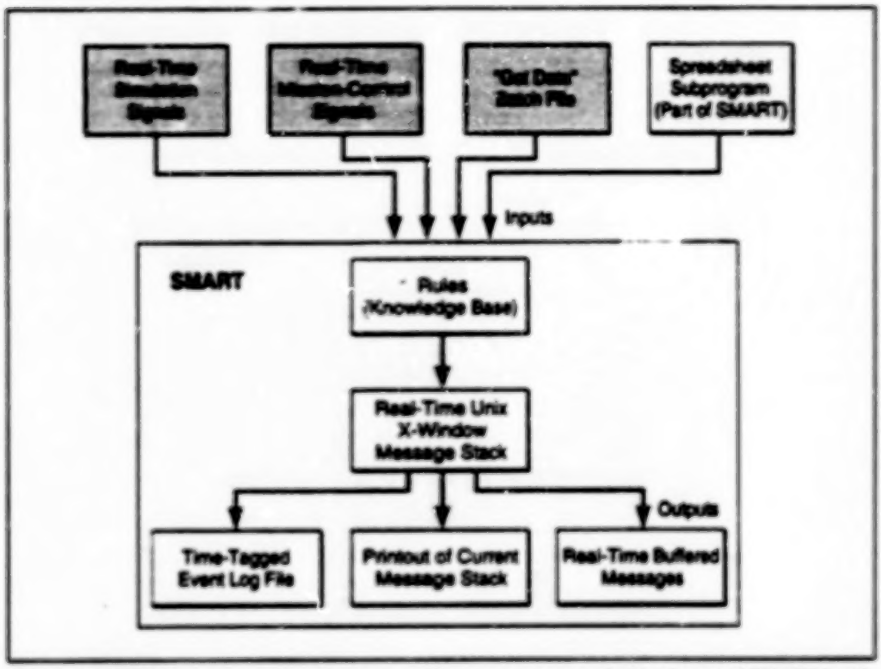


**Figure 1. SMART can receive input from any of four sources, one of which is part of SMART itself.**

Dryden Flight Research Center has developed a computer program that performs signal management for analysis in real time (SMART). This program, called "SMART," has been effectively used since 1991 in F-18, X-31, LASRE, and X-33 programs.

Figure 1 depicts the architecture of SMART. Signals are processed by executing rules (represented by Boolean expressions) that generate messages on a Unix X-Window. Inputs to SMART can come from any or all of several sources, as discussed below:

One of the sources can be a computational simulation. SMART is very effective for use in a simulation environment, because the simulation scripts can be used in conjunction with the rules to automate pass/fail criteria for software testing. Such raw words as signals on a 1553-standard bus are very easily decoded by SMART into meaningful textual character strings. As scripts are run, test words can be controlled to indicate to SMART that a particular test is being run. SMART generates the appropriate messages for the autotesting of the simulation software. All tests are exactly repeatable, very fast, and self-analyzing.

Another source of input to SMART can be a control room for an aircraft or spacecraft mission. The use of SMART during flight testing in such programs as the X-31 and LASRE has proven to be very valuable. For flight testing, safety of flight is the primary concern, and SMART works very well because health and status words are constantly being monitored. Status is not missed because when any fault is detected, a new colored (red) message is added to the top of a real-time Unix X-Window message stack. An additional benefit is that each such message is time-tagged. Data can be analyzed easily because

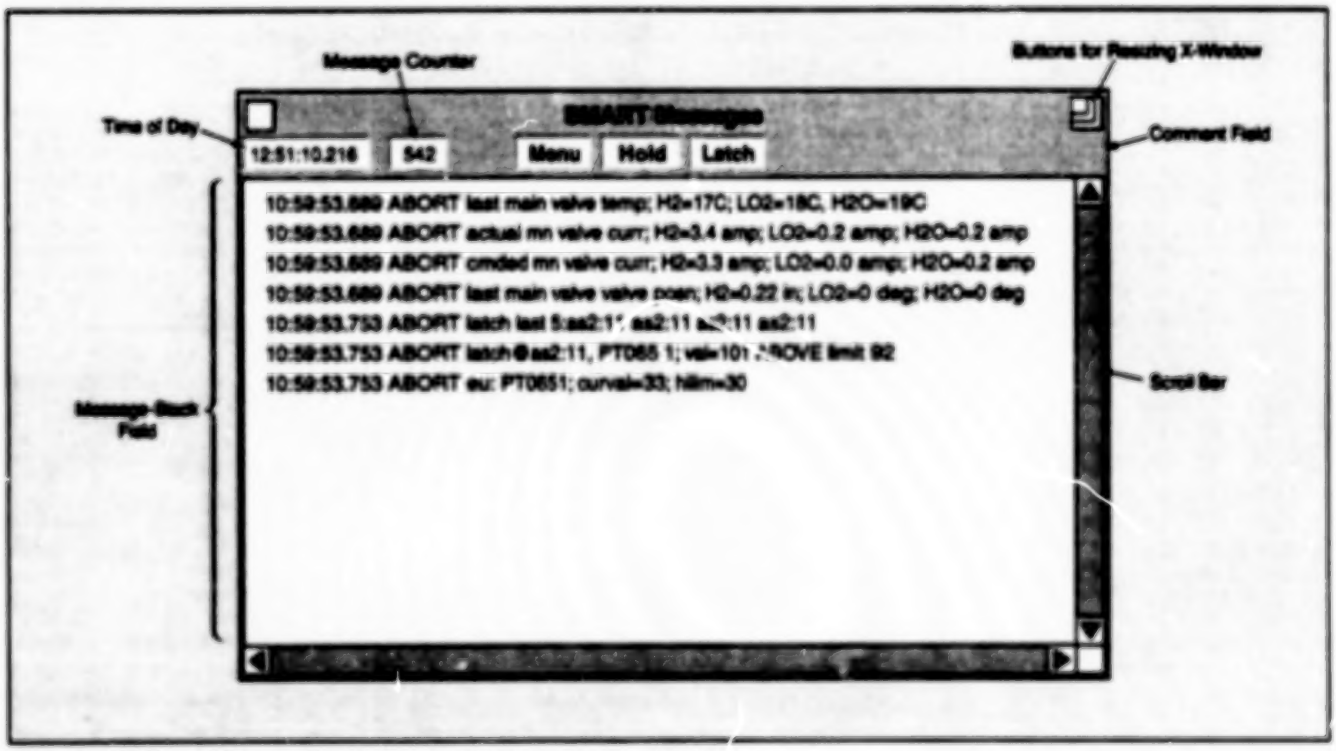
Message Counter
Buttons for Resizing X-Window
Time of Day
SMART Messages
Comment Field
12:51:10.216
542
Menu
Hold
Latch
10:59:53.689 ABORT last main valve temp; H2=17C; LO2=18C, H2O=19C
10:59:53.689 ABORT actual mn valve curr; H2=3.4 amp; LO2=0.2 amp; H2O=0.2 amp
10:59:53.689 ABORT cmded mn valve curr; H2=3.3 amp; LO2=0.0 amp; H2O=0.2 amp
10:59:53.689 ABORT last main valve valve posn; H2=0.22 in; LO2=0 deg; H2O=0 deg
10:59:53.753 ABORT latch last 5:as2:1*, as2:11 as2:11 as2:11
10:59:53.753 ABORT latch@as2:11, PT065 1; val=101 ABOVE limit 92
10:59:53.753 ABORT eu: PT0651; curval=33; hilim=30
Scroll Bar
Message-Stack Field

**Figure 2. A Dynamic Message Stack contains the primary output of SMART.**

SMART gives event times. All faults are immediately made known to enable quick action by a flight-test team.

A third source of input is a "GetData" batch file. The capability to receive data from this source is a recent addition to SMART. SMART reads the batch file, frame by frame, at whatever rate the data come in, and generates messages according to the rules. This capability is very effective in automating the analysis of batch data. Certain events can easily be tested by the rules and messages generated. It is also very helpful in developing the rules by use of known events representative of those that it is very important to be able to detect.

A fourth source of input is a spreadsheet subprogram that is part of SMART. This subprogram is used by a rules developer to test the rules. There is an option to automatically load all the signals from an input rule source onto a spreadsheet. The tester can click a cell and type the desired data value to test the rules. The message(s) appear on the stack when the rule has been satisfied.

The primary output of SMART consists of messages put into a dynamic stack. New messages are always added to the top of the stack and as old messages are rescinded, the stack is compressed to fill in the gaps. Messages can also be color-coded to enhance the visibility of designated information. The current messages in the stack can be sent to a printer at any time by use of a print command on the SMART window.

The SMART window provides an option to save the messages in a log file on a hard disk. This option is very useful for saving time-tagged event information for testing. Certain information can be scanned out from this file by use of standard Unix commands; this feature was found to be very useful in the LASRE program.

Another option, which was recently added to SMART, provides for triggering by a rule to generate a message and the current time and record the message and its time tag in a file. Information is continuously written into this file as long as the rule is satisfied. The message is defined by the developer. The message could be, for example, a parameter to be recorded whenever a fault flag is set. This option is meant to be used as a tool for analyzing anomalies as quickly as possible.

*This work was done by Richard Larson of* **Dryden Flight Research Center**. *Further information is contained in a TSP [see page 1].*
*DRC-99-28*

## Automated Generation of Acoustic-Propagation Computer Codes

Traditionally labor-intensive programming tasks are performed automatically by software.

*John H. Glenn Research Center, Cleveland, Ohio*

A computer program written within the Mathematica software system automatically generates FORTRAN computer codes that numerically simulate, with high accuracy, the acoustical physics of complex unbounded three-dimensional or bounded two-dimensional flow fields. The program is a significant contribution to the field of computational aeroacoustics (CAA), which combines the traditional disciplines of acoustics and computational fluid dynamics (CFD). The program was developed, as a first step, to accelerate and facilitate analysis of noise generated by turbofan aircraft engines. It can also be applied in many other endeavors that involve the generation, propagation, and/or scattering of electromagnetic as well as acoustic waves, or in which there are requirements to obtain highly accurate solutions of systems of hyperbolic partial differential equations that describe physical phenomena in complex environments. Prior to the development of this program, considerable programming effort was necessary even to obtain a low-accuracy computer code for a typical application. The code generated automatically by this program is far more accurate and efficient.

In the original turbofan-noise application, there is a need for numerical-simulation software that has sufficient fidelity to simulate steep gradients in flow fields and that is efficient enough to run on today's computer systems. The present code-generator program was developed to satisfy this need and, more specifically, to create software that numerically solves the linearized Euler equations of flow on Cartesian grids in three-dimensional spatial domains that contain bodies with complex shapes.

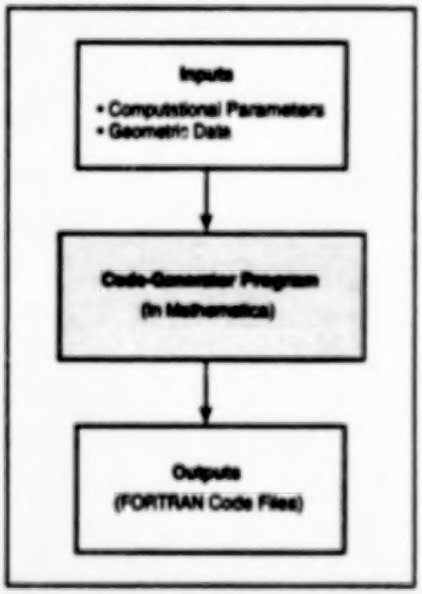


**Once the Problem Is Specified** in terms of computational parameters (e.g., numbers of grid points) and geometric data, the FORTRAN code files needed to solve the problem are generated automatically.

The codes are based upon the recently developed Modified Expansion Solution Approximation (MESA) series of explicit finite-difference schemes. The essential idea behind the MESA schemes is to approximate the solutions of the partial differential equations instead of approximating the individual derivative terms. The MESA schemes use multidimensional spatial interpolation and the constructive procedure in the proof of the Cauchy-Kovalevsky theorem to develop a local series approximation to the solution of the system of partial differential equations in both space and time. MESA schemes provide spectrallike resolution with extraordinary efficiency and can, theoretically, offer levels of accuracy that are arbitrarily high in both space and time, without the inefficiencies of Runge-Kutta schemes. The MESA methods were originally developed in one and two dimensions with accuracy up to 11th order, but, in conjunction with the development of the present program, have been extended to three dimensions with accuracy up to 29th order in space and time.

Unfortunately, the complexity of the coding task in the original form of the MESA schemes was very high, so that in a given application, either the desired code could not be compiled or else it took an impractically long time to write the code in FORTRAN. The present code-generator program automatically codes the MESA schemes into FORTRAN. As part of the development of this program, the MESA schemes were reformulated into a very simple form, making it practical to use

these schemes without the automation or, alternatively, making these schemes very powerful when the automation is used. The program provides means for treating grid-aligned solid wall boundaries in two dimensions with accuracy up to 11th order, and for treating generalized two-dimensional boundaries with accuracy up to second order. It also provides for automated parallelization of codes for execution on large-scale parallel computers.

This program is a "turnkey" code-generation software tool. Given input in the form of computational parameters plus a set of parametric curves that describe the object(s) that bound a flow field, the program automatically generates the code that simulates the acoustical physics of the flow field. The program thus relieves engineers and scientists of the traditionally labor-intensive tasks of generating computational grids, developing algorithms to solve the governing differential equations, coding the algorithms in FORTRAN, and ensuring that wall boundaries are treated correctly. By shifting these tasks to computers, the program can be expected to increase its users' productivity and capability. Additional work is required, however, to fully simulate bounded three-dimensional problems.

*This work was done by Rodger W. Dyson and John W. Goodrich of* **Glenn Research Center**. *Further information is contained in a TSP [see page 1].*

*Inquiries concerning rights for the commercial use of this invention should be addressed to NASA Glenn Research Center, Commercial Technology Office, Attn: Steve Fedor, Mail Stop 4–8, 21000 Brookpark Road, Cleveland, Ohio 44135. Refer to LEW-16970.*

# END

# 09-12-00